Mineral Reconnaissance Programme Report

D. Ostle
Programme Manager
Institute of Geological Sciences
Keyworth,
Nottingham NG12 5GG

No. 48

Mineral investigations near Bodmin, Cornwall

Part 3– The Mulberry and Wheal Prosper area

Mineral Reconnaissance Programme

Report No. 48

Mineral investigations near Bodmin, Cornwall

Part 3—The Mulberry and Wheal Prosper area

Geology
M. J. Bennett, BSc, ARSM
K. E. Beer, BSc, CEng, FIMM

Geochemistry
R. C. Jones, BSc
K. Turton, BA

Geophysics
K. E. Rollin, BSc
J. M. C. Tombs, BSc
D. J. Patrick, BSc, PhD

Mineral Reconnaissance Programme Reports

1　The concealed granite roof in south-west Cornwall

2　Geochemical and geophysical investigations around Garras Mine, near Truro, Cornwall

3　Molybdenite mineralisation in Precambrian rocks near Lairg, Scotland

4　Investigation of copper mineralisation at Vidlin, Shetland

5　Preliminary mineral reconnaissance of Central Wales

6　Report on geophysical surveys at Struy, Inverness-shire

7　Investigation of tungsten and other mineralisation associated with the Skiddaw Granite near Carrock Mine, Cumbria

8　Investigation of stratiform sulphide mineralisation in parts of central Perthshire

9　Investigation of disseminated copper mineralisation near Kilmelford, Argyllshire, Scotland

10　Geophysical surveys around Talnotry mine, Kirkcudbrightshire, Scotland

11　A study of the space form of the Cornubian granite batholith and its application to detailed gravity surveys in Cornwall

12　Mineral investigations in the Teign Valley, Devon. Part 1—Barytes

13　Investigation of stratiform sulphide mineralisation at McPhun's Cairn, Argyllshire

14　Mineral investigations at Woodhall and Longlands in north Cumbria

15　Investigation of stratiform sulphide mineralisation at Meall Mor, South Knapdale, Argyll

16　Report on geophysical and geological surveys at Blackmount, Argyllshire

17　Lead, zinc and copper mineralisation in basal Carboniferous rocks at Westwater, south Scotland

18　A mineral reconnaissance survey of the Doon-Glenkens area, south-west Scotland

19　A reconnaissance geochemical drainage survey of the Criffel-Dalbeattie granodiorite complex and its environs

20　Geophysical field techniques for mineral exploration

21　A geochemical drainage survey of the Fleet granitic complex and its environs

22　Geochemical and geophysical investigations north-west of Llanrwst, North Wales

23　Disseminated sulphide mineralisation at Garbh Achadh, Argyllshire, Scotland

24　Geophysical investigations along parts of the Dent and Augill Faults

25　Mineral investigations near Bodmin, Cornwall. Part 1-Airborne and ground geophysical surveys

26　Stratabound barium-zinc mineralisation in Dalradian schist near Aberfeldy, Scotland: Preliminary report

27　Airborne geophysical survey of part of Anglesey, North Wales

28　A mineral reconnaissance survey of the Abington-Biggar-Moffat area, south-central Scotland

29　Mineral exploration in the Harlech Dome, North Wales

30　Porphyry style copper mineralisation at Black Stockarton Moor,south-west Scotland

31　Geophysical investigations in the Closehouse-Lunedale area

32　Investigations at Polyphant, near Launceston, Cornwall

33　Mineral investigations at Carrock Fell, Cumbria. Part 1-Geophysical survey

34　Results of a gravity survey of the south-west margin of Dartmoor, Devon

35　Geophysical investigation of chromite-bearing ultrabasic rocks in the Baltasound-Hagdale area, Unst, Shetland Islands

36　An appraisal of the VLF ground resistivity technique as an aid to mineral exploration

37　Compilation of stratabound mineralisation in the Scottish Caledonides

38　Geophysical evidence for a concealed eastern extension of the Tanygrisiau microgranite and its possible relationship to mineralisation

39　Copper-bearing intrusive rocks at Cairngarroch Bay, south-west Scotland

40　Stratabound barium-zinc mineralisation in Dalradian schist near Aberfeldy, Scotland: Final report

41　Metalliferous mineralisation near Lutton, Ivybridge, Devon

42　Mineral exploration in the area around Culvennan Fell, Kirkcowan, south-western Scotland

43　Disseminated copper-molybdenum mineralisation near Ballachulish, Highland Region

44　Reconnaissance geochemical maps of parts of south Devon and Cornwall

45　Mineral investigatons near Bodmin, Cornwall. Part 2— New uranium, tin and copper occurrence in the Tremayne area of St Columb Major

46　Gold mineralisation at the southern margin of the Loch Doon granitoid complex, south-west Scotland

47　An airborne geophysical survey of the Whin Sill between Haltwhistle and Scots' Gap, south Northumberland

48　Mineral investigations near Bodmin, Cornwall. Part 3—The Mulberry and Wheal Prosper area

CONTENTS

SUMMARY

Investigations in the area between the former open-cast tin workings of Mulberry and Wheal Prosper suggest that the most promising ground for future mineral exploration lies to the south of the latter workings. The north-south Mulberry mineralisation trend, although recognisable south of the calc-silicate belt, gives rise to only sporadic and low-amplitude tin anomalies in the soils. Near to the surface there is no evidence of an analogue of the Mulberry deposit; its existence or absence at depth could only be proved by speculative drilling. Traced westwards, the Prosper mineralisation becomes more tenuous and, at shallow depth, un-economic.

Strong geochemical evidence, supported by less firm geophysical indications, points to the presence of a previously unrecognised mineralised zone sub-parallel to the Prosper vein sheets and some 200 m south of them. The presence of tin, copper, zinc and a little tungsten is indicated.

INTRODUCTION

Although the so-called stockwork tin deposits of Mulberry [c. SX 020 658] *, Wheal Prosper [c. 030 642] and Criggan [015 610] (Figures 1 and 2) were worked periodically until early in this century and individually have attracted attention since then, there is no record of serious exploration in the ground between them. The initial purpose of the current investigation was to remedy this omission.

Early geochemical reconnaissance traverses showed no promise in the southern part of the area and subsequent activity was concentrated around Wheal Prosper. Here the land is devoted entirely to mixed farming and evidence of former mining activities is being eradicated slowly by the removal of waste dumps and infilling of shafts and quarries. The Mulberry and Prosper workings occur on relatively high ground in a generally broadly un-dulating topography (Figure 1). In the north the stream valleys are usually narrow and deeply cut but in the south they are marked by wide stretches of scrub-covered alluvium. The area is well served by a network of generally narrow lanes leading off the A30 trunk road from Bodmin to Redruth.

*All locations in this report lie within 100 km National Grid square SX.

GEOLOGICAL SETTING

The area examined is largely underlain by sedi-ments of the Meadfoot Beds, of Lower Devonian age, though the Criggan tin working lies just within the St Austell Granite (Figure 2). Exposure is poor over much of the area but the harder bands of calc-silicate rocks and the elvan dykes were formerly quarried for road and building stone.

The Meadfoot Beds consist predominantly of variably grey slates, usually colour banded and commonly slightly calcareous. Sandier horizons occur here and there and become particularly abundant towards the top of the succession as the Staddon Grits are approached. South of the A30 road the sediments are generally thermally meta-morphosed, field brash showing all gradations from slates to tough hornfelses. Tourmalinisation of the slates is common and locally may be very intense with the development of a banded quartz-schorl rock. Only occasional spotting is seen north of the road and this is confined to particular silty litholo-gies.

A low ridge between the Mulberry openwork and Higher Woodley [022 648] marks the outcrop of east—west bands of calc-silicate rocks (calc-flintas). Although usually green or greenish grey, these rocks may display a wide range of colours and an equally wide range of grain sizes. Fine-grained varieties are notably siliceous and flint-like, often finely banded and brittle, with a conchoidal fracture. The coarser variants are distinctly granu-lar and composed mainly of well-crystallised garnet with green amphibole, diopside, actinolite, chlo-rite, a little quartz or feldspar and occasional cal-cite. Their variation and distribution is well described by Barrow (in Ussher and others, 1909) but, somewhat surprisingly, they have received scant attention since that time.

Some bands, particularly those in which the amphibole is chloritised, contain disseminated sphalerite, chalcopyrite and arsenopyrite and rarely these ore minerals are highly concentrated in beds up to 3 cm thick. By far the commonest mode of mineralisation, however, is as networks of fine veinlets. In boreholes drilled by Consolidated Goldfields Ltd. some of the calc-silicate horizons were shown to carry cassiterite, both as fine dis-seminations and as narrow tension-gash fillings; the garnets were also stanniferous.

The calc-silicate rocks represent highly meta-somatised sediments, the original composition of which was probably widely variable, encompassing
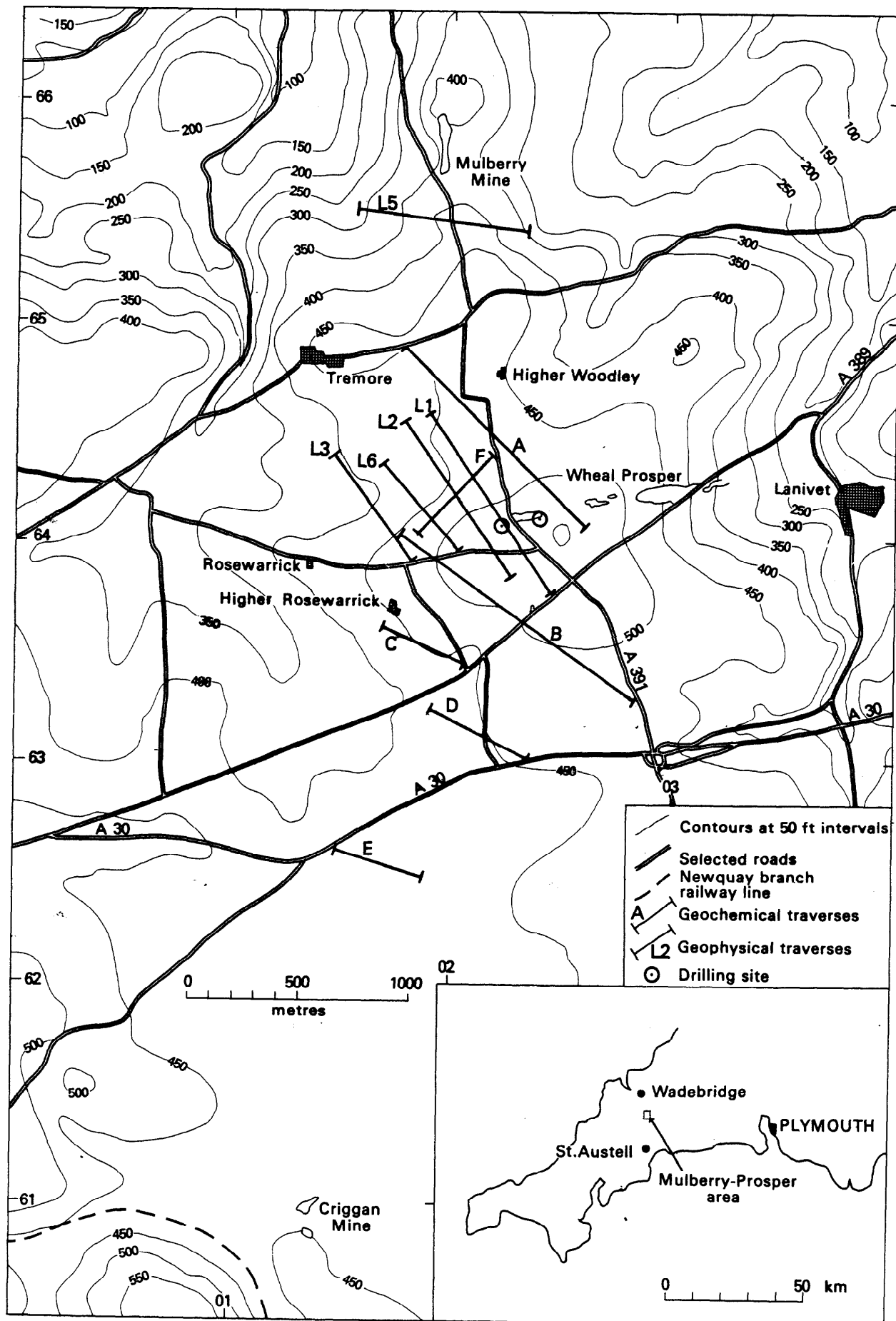
Fig.1 Location of the Mulberry-Prosper area

Fig.2 Geology of the Mulberry-Prosper area
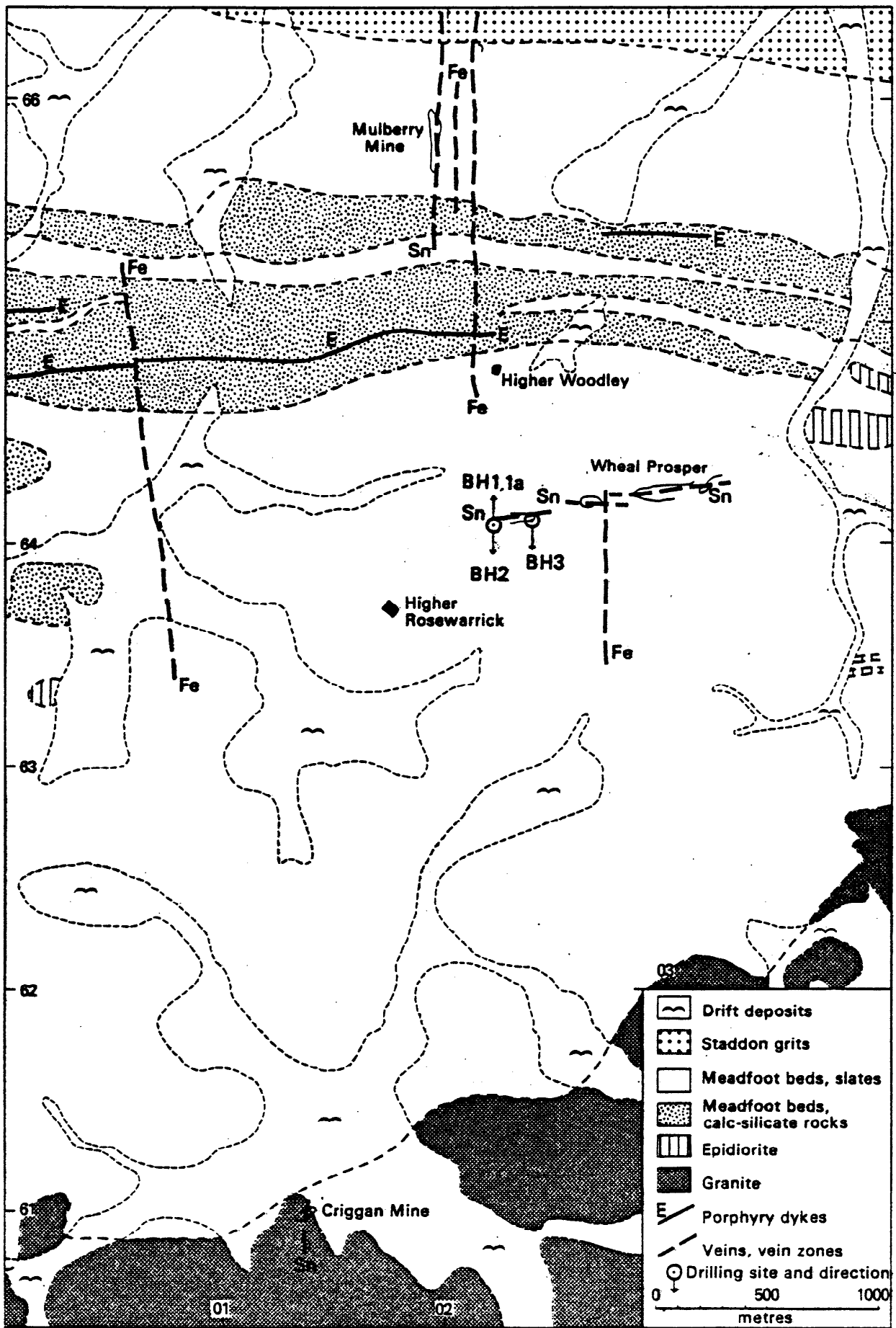
Legend:

- ∿ Drift deposits
- Staddon grits
- Meadfoot beds, slates
- Meadfoot beds, calc-silicate rocks
- Epidiorite
- Granite
- E⟋ Porphyry dykes
- ⟋ Veins, vein zones
- ⊙↓ Drilling site and direction

Scale: 0 — 500 — 1000 metres

a range of limestones, marls, tuffs and cherts and perhaps including thin greenstone sills. Accepting that the metasomatic fluids derived their heat and at least some of their reactive constituents from the granite, the location of this calc-silicate belt well outside the normal thermal aureole may be taken to indicate the presence of an underlying (east-west?) granite ridge. Barrow (*op. cit.*, p. 86) places this immediately north of the Tremore quarries, i.e. at about the latitude of the Mulberry pit. Recent gravity modelling, however, suggests no hidden cuspate granite at this latitude, though it does indicate a rise in the granite roof below the Prosper quarries. It is pertinent to record that the commercial boreholes at Mulberry showed no evidence of thermal metamorphism at depth.

Within the Mulberry openwork, the Meadfoot Beds slates dip at about 45° to the north but in the eastern quarry of Wheal Prosper the dip is southerly and considerably steeper (60° or more). The calc-silicate bands, therefore, appear to occupy the exposed axial core of a regional anticlinorium but within their outcrop several folds with smaller amplitudes can be recognised.

The investigation was not carried into the granite country in the south of the area. Around Criggan Mine near-surface kaolinisation is locally well developed and has been worked in several small china clay pits, but at the mine the host rock is reported as being hard (Dines, 1956).

Three elvan dykes occur in the study area; all trend east—west and lie within the calc-silicate outcrop. The most continuous elvan has been quarried just west of Tremore [014 648] and yielded an attractive building stone. It is locally affected by metasomatism, being traversed by axinite-amphibole veins with marginal developments of borosilicates in the fissure walls. The Retire Iron Lode also cuts this elvan, displacing it slightly and locally pervading it with iron oxides.

Three types of mineralisation are known in the area and all have been worked in the past. Cassiterite, with minor sulphides and traces of wolframite, occurs as closely-spaced narrow fissure fillings and thin veinlets at Mulberry, Prosper and Criggan. The sheeted veins of Wheal Prosper trend approximately east—west, those of Mulberry and Criggan approximately north—south (Figure 2). All have been worked over limited strike lengths and narrow widths, the extent of the workings being dependent upon the frequency of veinlets and bulk grade of the ore. Typically the veinlets are composed of quartz with selvages of mica and tourmaline — the greisen-bordered veinlets of Hosking (1969) which, he suggests, were preferentially developed over granite cusps and were emplaced early in the regional mineralisation sequence. Within the veinlets cassiterite is widely scattered as coarse and often euhedral crystals; stannite is also present in these veins.

Two east—west copper veins are recorded at Wheal Betsy [010 647], just west of Tremore.

There are no records as to the nature of this or other apparently similar copper structures reported in the Tremore valley but from the sketchy mine section it appears that the orebody was of very limited extent.

Late north—south hematite lodes have been worked west of the Tremore valley, immediately east of Mulberry openwork and south of Wheal Prosper. These structures are seen to cut the Prosper tin veins, and probably to displace them, and are reported to cut east—west copper veins in Wheal James [c. 007 648]. Brown hematite is the major constituent of these lodes but locally manganese oxides are particularly abundant. There is a scattering of fine sulphides in some of the ore and occasional clusters of green uranium secondary minerals. In a sample from the Wheal James adit dumps anomalously high selenium was found. Dines (1956) maintains that the hematite ore is an oxidation product of primary siderite but some of the textures seen in the ore do not support this thesis.

FORMER MINING AND EXPLORATION

The mining history of this area is imperfectly known and its resolution is further confused by a multiplicity of similar mine titles for which accurate sites cannot be deduced (Jenkin, 1964a). Mulberry openwork is shown on maps as early as 1748 but nothing is known of its early production. Output figures for all the mines are sketchy and date only from the mid-19th century.

Mulberry openwork is about 275 m long, 40 m wide and up to 36 m deep. From this hole about one million tonnes of rock have been removed which, at an estimated grade of 0.30% Sn (Dines, 1956), should have yielded about 2,400 tonnes of tin-in-concentrate (assuming c. 80% recovery). Records, however, show only 1330 tonnes of black tin (c. 870 tonnes Sn) returned in the period 1859 to 1908 (Collins, 1912) during intermittent operation. The openwork was last worked in 1914, though it has attracted attention since.

Separate tin workings seem to have operated to the east and south-east of the pit but there is confusion arising from similarities of naming. Through this uncertainty, however, there persists a belief that more 'ore ground' exists to the east of the pit and similar claims are made for the area to the west of the pit (Dines, *op. cit.*). Prior to 1940 some prospecting trenches north of the openwork reported grades of up to 0.53% Sn but no development ensued.

In the 1960's, following a geochemical soil sampling study conducted by Dr K.F.G. Hosking, Consolidated Goldfields Ltd. drilled 15 inclined boreholes to investigate the lateral and depth extension of the mineralisation. Short boreholes were also drilled sub-horizontally from the tramming level below the openwork floor. Tin veining

4

was shown to continue in depth over the full width of the opencast and at a comparable grade to that reported historically. A little wolfram, copper sulphides and native copper was also encountered. To the north of the pit indications were less promising but to the south continuity of mineralisation was traced into the calc-flintas, where the cassiterite was more widely disseminated, though at unimproved grade overall. After Consolidated Goldfields Ltd. relinquished their lease, four more short holes were drilled into the calc-flintas by Noranda Kerr Ltd. and proved low-grade tin mineralisation.

Wheal Prosper is the collective name for four quarry openworks operated intermittently for tin in the period from 1846 to 1928. Each quarry was separately titled — South Woodley, Wheal Sara, Wheal Prosper and Wheal Michell, from west to east. The largest working was Wheal Prosper from which some 2 million tonnes of ore were extracted at a grade of only 0.13% Sn. Grades in South Woodley and Sara were at least twice this level. Such poor ore was only viable by virtue of the soft host slates and the coarseness and cleanliness of the cassiterite content — only traces of sulphides and wolfram are found in the veinlets.

The Prosper group was attracting interest in about 1951 but no exploration was undertaken. The intersection of the Mulberry and Prosper trends was not examined in the 1960s.

Criggan Mine, also known as Carrigan Consols, worked a zone of sheeted tin-bearing quartz veins in greisen to a depth of about 18 m by opencast methods and thereafter followed them a further 30 m by small-scale mining (Jenkin, 1964b). This work was completed by 1839 but the openwork was restarted and expanded between 1874 and 1885. According to Collins (1912) the mineralised greisen zone was 90 m long and 45 m wide with a grade of about 0.25% Sn. So far as is known this deposit has attracted no further attention during this century.

Most of the alluvium in the study area has been turned over for stream tin at some past date. Virtually nothing is known of these operations but it may be anticipated that some cassiterite, particularly the finer sizes, still remains.

Little is known about Wheal Betsy (or Betsy and Penvivian) save that it was working in about 1857, developing two lodes by adits and a single shaft. A small area of stoping around this shaft (on North Lode?) extends about 6 fathoms (11 m) below adit level. Pitchblende was reported from a lode near Tremore, perhaps from this mine (Mining Journal, 19.9.1857).

The iron lode west of the Tremore valley was worked by four mines — Wheal James, Retire Mine [007 646], Rosewarrick Mine [007 639] and Colbiggan Mine [008 636] from north to south — and at various dates these combined under differing titles. Mining began before 1845 and continued to about 1875. Torbernite was reported in the 1850s and was said to come from intersections of the iron lode with east—west copper lodes. Uraniferous waste is fairly widely scattered at surface, however, and may indicate a less confined distribution within the iron ore. The Atomic Energy Division of the Geological Survey attempted to reopen the Wheal James adit in 1957 but was defeated by unstable wall conditions.

Similar iron lodes, though not known to be uraniferous, were worked north-west of Higher Woodley and south of Prosper. The latter lode, worked as Westdowns (or Bigbees) Mine [027 635], was followed northwards into Wheal Sara quarry where it cuts (and displaces?) the east—west tin structures. Records of iron production are incomplete and the habit of bulking returns from scattered mines further confuses the issue. That the output was considerable can be in little doubt as a mineral branch line was constructed to transport the ore from Wheal James adit to the Wadebridge line at Ruthernbridge [013 668]. A spur from this branch served the Mulberry dressing plant near Cork farm [014 662]. The iron ores were reported upon comprehensively by Groves (1941) but have received no attention since.

GEOCHEMICAL INVESTIGATIONS

RECONNAISSANCE TRAVERSES

The initial geochemical soil survey consisted of six traverses, designated A to F (Figures 1,3 and 4), incorporating 177 samples taken at 25 m intervals from the C-horizon at depths from 0.25 to 1.0 m. The pattern of traverses was intended to provide the fullest coverage of the Mulberry, Prosper and Criggan vein trends and the north—south West Downs Iron Lode extension, whilst avoiding as far as possible the cassiterite-bearing alluvium north of Higher Rosewarrick [017 637]. Traverses were orientated north-west—south-east or north-east—south-west to intersect both trends at a favourable angle.

All samples were sieved at 60 B.S.S. mesh and the fines ground to 200 B.S.S. size prior to analysis for Cu, Sn, W and As.

RESULTS

Tin-tungsten (Figure 3): Traverse A highlights two areas of elevated tin and tungsten values. To the west of Higher Woodley tin levels reach 500 ppm and tungsten 50 ppm in a broad anomaly near the boundary between Meadfoot Beds slates and calc-silicate rocks and on the trend of the Mulberry mineralisation. Increasing Sn and W values within the calc-silicate outcrop may reflect dispersed mineralisation of the type encountered in some of the Consolidated Goldfields boreholes. Between the former openworks of Wheal Prosper there is a major anomaly, 250 m in width, with tin values up to 700 ppm and tungsten to 120 ppm. Although

CALC SILICATES

Sn

65

W

Higher Woodley

CALC SILICATES

SLATES

SLATES

Sn

F

W

Sn

Wheal Prosper

A

BODMIN

64

Sn

W

Higher
Rosewarrick

Sn

W

West Downs
Iron Mine

C

B

Sn

W

TRURO

D

LANIVET

63

0   500
metres

700

Sn
ppm

100

50
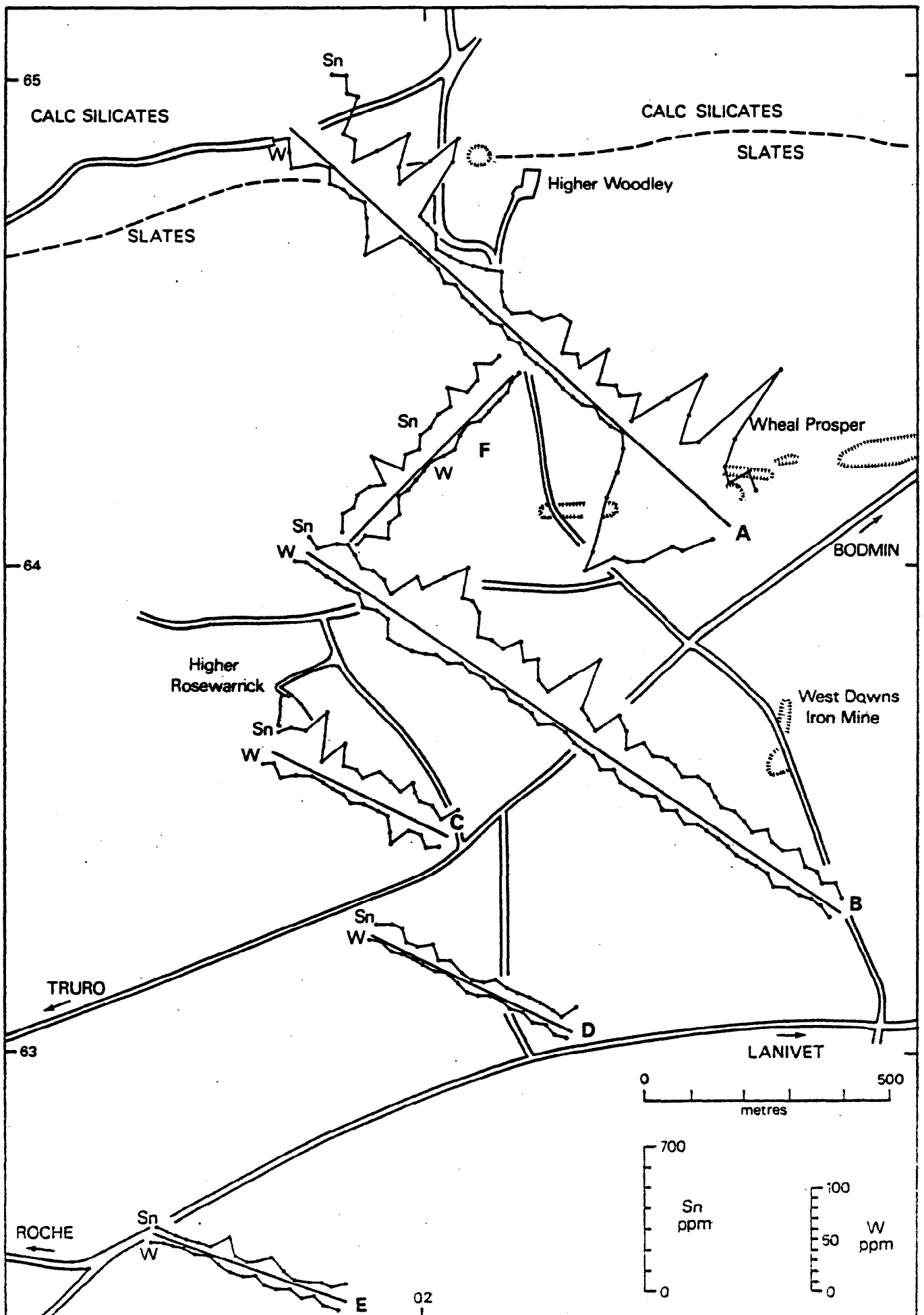
0

W
ppm

ROCHE

Sn

W

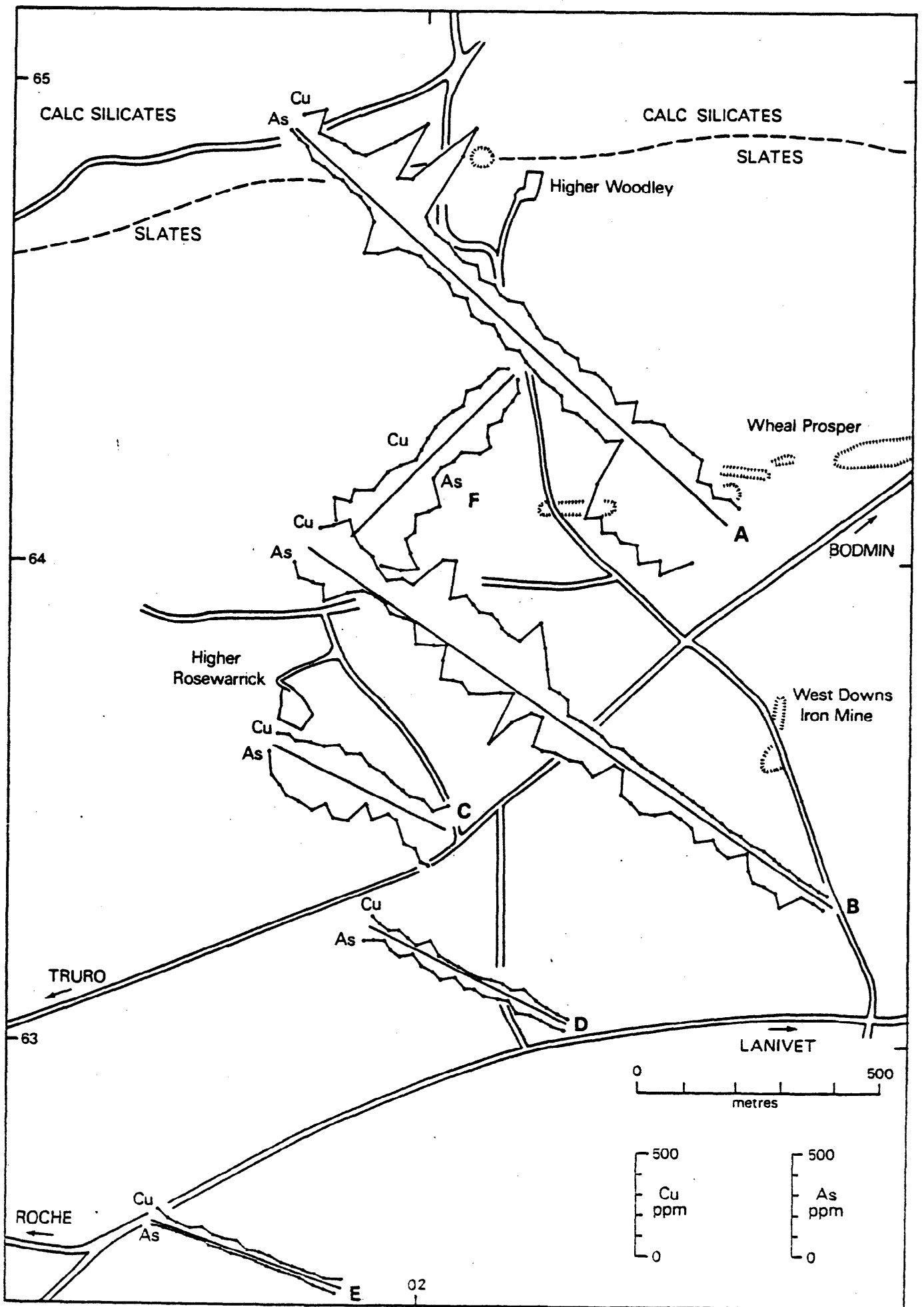E   02

0

Fig. 3 Tin and tungsten in soil samples

6

Fig. 4 Copper and arsenic in soil samples

undoubtedly representing in-situ mineralisation, these values are probably enhanced by contamination from scattered mining debris; fragments with joint faces coated by cassiterite and rare wolframite can be collected from the field float.

Along traverse B there are two tin anomalies neither of which is accompanied by significantly elevated tungsten values. The more northerly one could be interpreted as representing an extension of the Mulberry trend, though there is little supporting evidence from traverse F. The southern anomaly does not correlate with any known mineralisation.

Traverses C and F show only minor localised anomalies; that at the western end of traverse C may be a lateral equivalent of the southern anomaly on traverse B. Only background values are recorded along traverses D and E.

Copper-arsenic (Figure 4): Along traverses A and F background values for both copper and arsenic are about 100 ppm. Towards the northern end of traverse A there is a double copper peak, the southern part of which correlates with a small arsenic peak. This may be regarded as a reflection of the Mulberry mineralisation trend and the arsenic-free northern part as an indication of disseminated copper mineralisation in the upper layers of the calc-silicate zone. The Prosper vein swarm is represented by a broad major arsenic anomaly at the southern end of traverse A. Significantly, this is not accompanied by anomalous copper though the presumed western extensions of this zone, seen as small anomalies at the southern end of traverse F and the western end of traverse B, do show small copper enrichments.

Elsewhere along traverse B the sharp arsenic peak just north of the Bodmin-Truro road correlates fairly closely with the tin anomaly previously reported and the more easterly copper peak is marginal to this. The copper anomaly close to the Higher Rosewarrick lane may be due to contamination. South of the Bodmin-Truro road background copper levels fall dramatically to less than 50 ppm and this level is further displayed in traverses D and E. Arsenic levels fluctuate considerably in traverse B but progressively fall southwards to a uniformly low level of 50 ppm or less.

In traverse C both copper and arsenic show generally elevated values but no discrete anomalies; neither do they correlate significantly with tin and tungsten levels.

SOIL GRID

Collection of soil samples on a rectangular grid pattern was carried out in two stages in order to avoid damage to growing crops and, unfortunately, the two batches of samples were analysed by different techniques. The coverage of sampling is shown in Figure 5; in a primary 150 × 150 m grid with partial infilling the standard station separation is 30 m.

All samples were taken from the C-horizon at depths of 0.5 to 1.0 m and after screening at 60 B.S.S. and grinding to −200 B.S.S. were analysed for Sn, W, Cu, Pb and Zn.

RESULTS

Copper: A total of 638 samples were analysed for copper, part by atomic absorption spectrophotometry (AAS) and part by X-ray fluorescence (XRF) analysis. The results were processed separately, but cumulative frequency plots (Figures 6 and 7) indicate adequate compatibility to permit combination into a single anomaly plot (Figure 8).

The cumulative frequency curve for AAS results shows no distinct population sets below 300 ppm, but that for XRF results has significant flexures at 80 and 170 ppm. For meaningful display, therefore, the copper distribution map was contoured at 100 ppm intervals commencing at the 150 ppm level.

Six small low-amplitude anomalies west of Higher Woodley lie close to the Mulberry trend axis and all except the southernmost anomaly also lie near the electricity power line. It is probable, therefore, that five of these may be caused by local man-made contamination. This area has been covered only by the broad grid and further sampling would be required to define the anomalies more precisely.

A broad area east and north-east of Higher Rosewarrick exhibits anomalously high values of copper in soils. Satellite anomalies at I and II (Figure 8) probably reflect the westward continuation of the Prosper mineralisation and correlate well with the primary traverse results. The major anomalies, however, lie some 100 m south of the Prosper axis and are themselves aligned almost east—west, subparallel to that axis. The central anomaly, at IV, lies suspiciously close to the line of the overhead transmission line and may be influenced by contamination. This is not the case at III, location of the highest anomaly (670 ppm), nor at V, and it may be speculated that these three anomalies reflect a narrow copper-bearing structure parallel to the Prosper trend. The apparent lack of continuity westwards is accentuated by the sparsity of sampling in this direction but, if genuine, is probably indicative of a cut off by the Mulberry trend or of a westerly plunge to the causative mineralisation.

Zinc: 520 samples were analysed for zinc by AAS and XRF techniques. Cumulative frequency plots for analyses by the two methods (Figures 9 and 10) were sufficiently similar below 600 ppm for the results to be plotted on one distribution map (Figure II). A contour interval of 100 ppm was adopted and a background level of 150 ppm.

The zinc anomalies fall conveniently into three groups. The highest zinc values are located west of Higher Woodley and reach a level of 11,000 ppm centred beneath the overhead power cable and
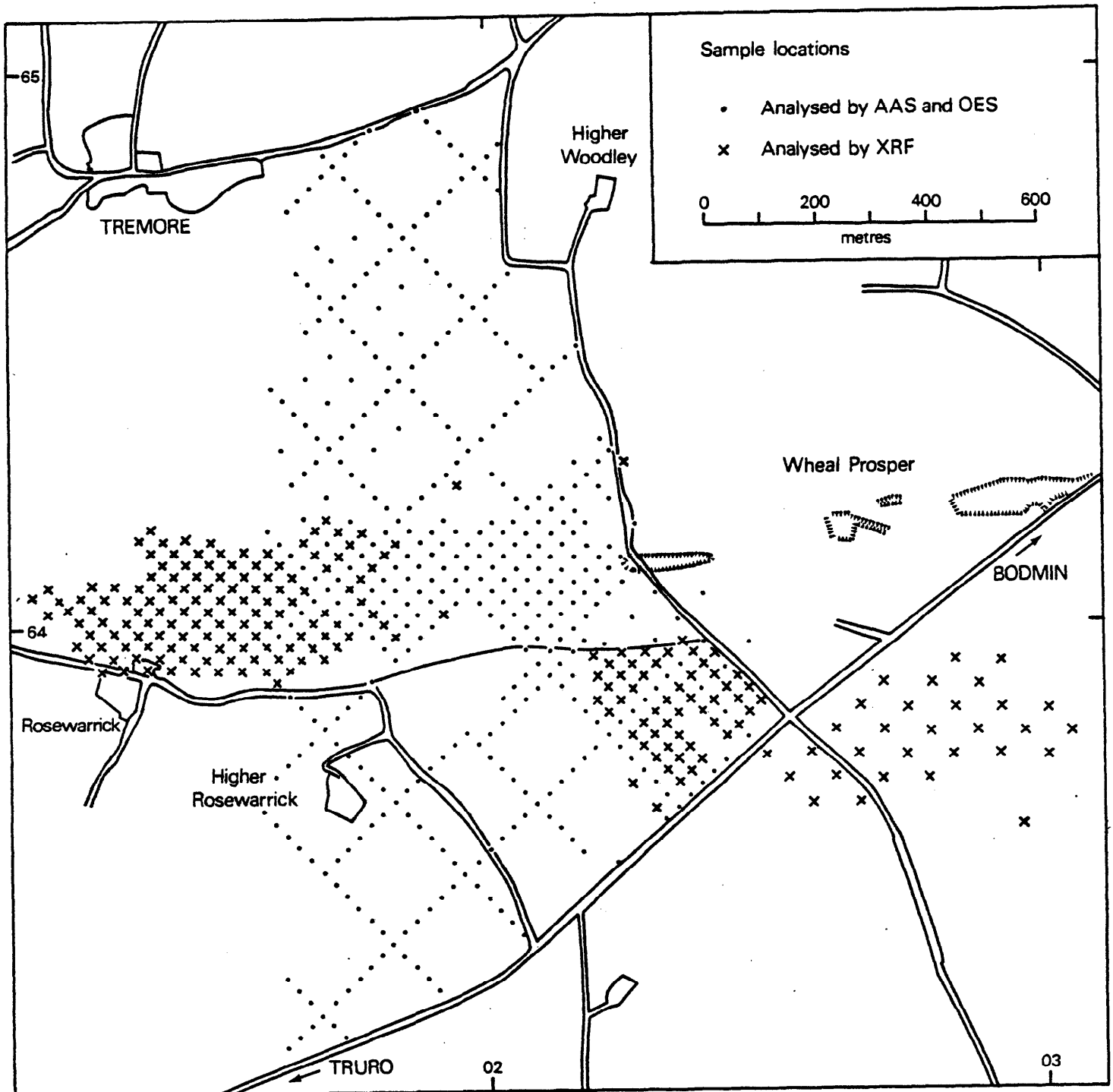
Fig. 5 Soil sampling grid
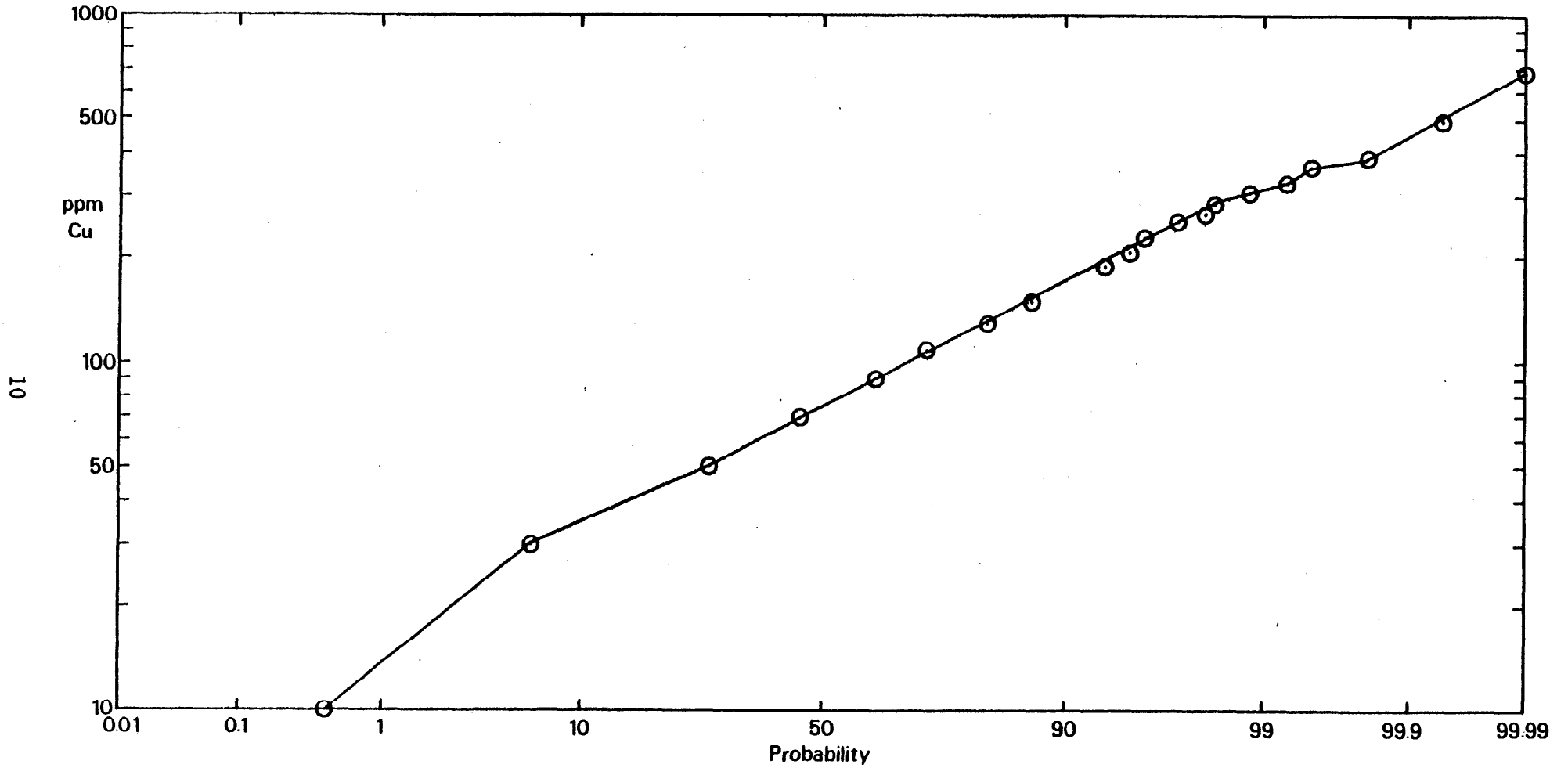
Fig. 6 Cumulative frequency plot for copper (A.A.S.)
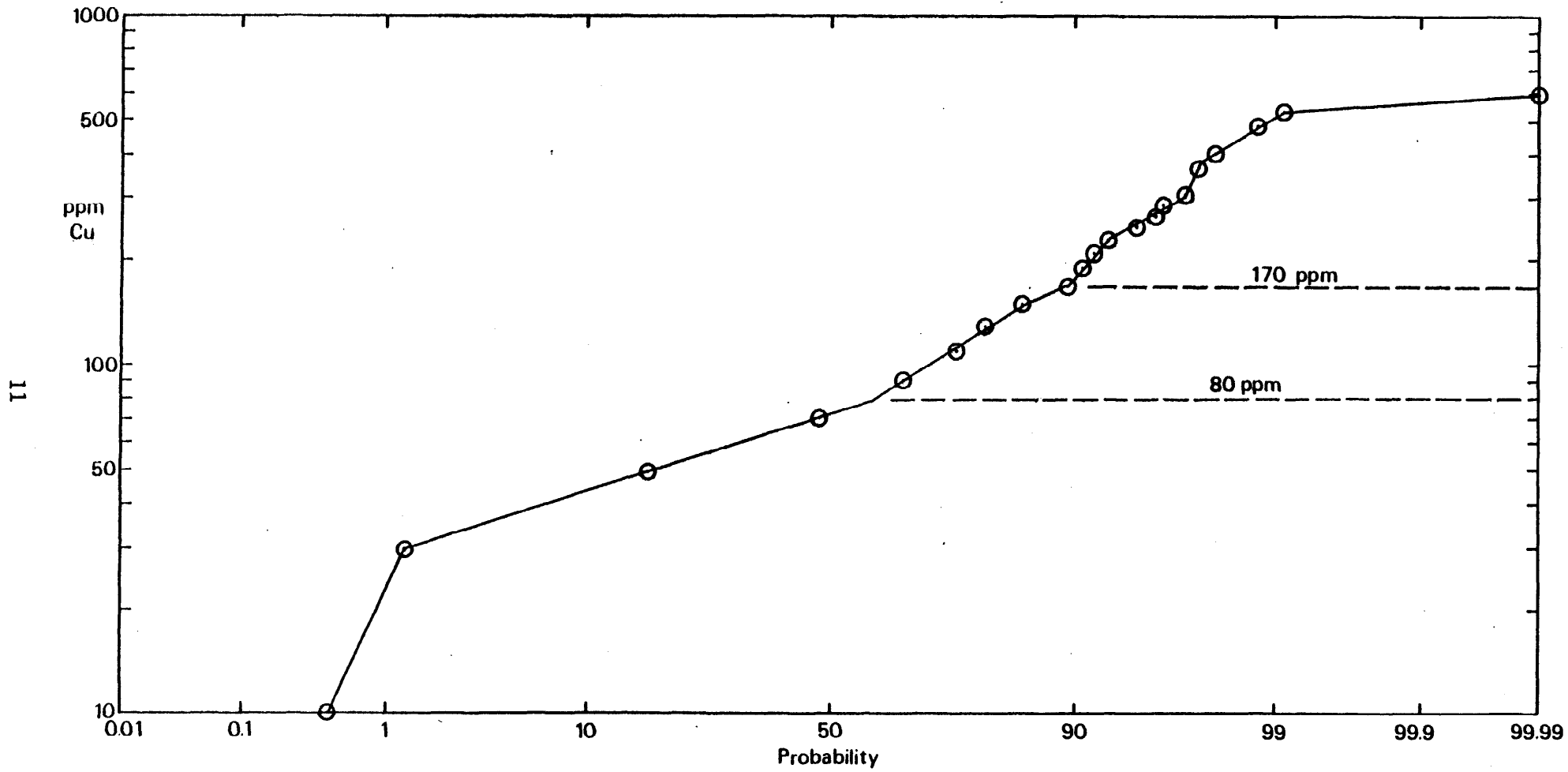
Fig. 7 Cumulative frequency plot for copper (X.R.F.)
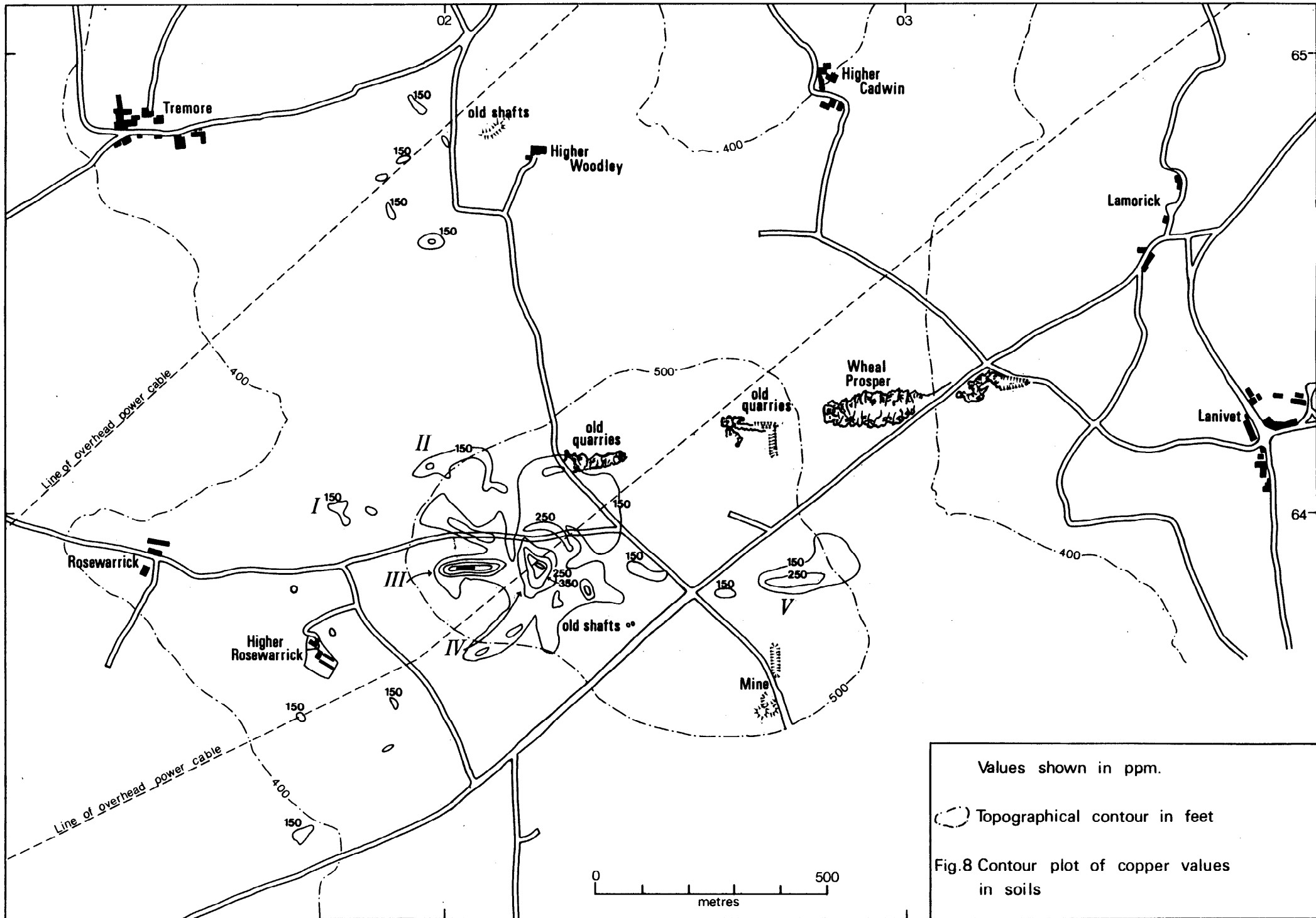
Fig.8 Contour plot of copper values in soils

Values shown in ppm.

Topographical contour in feet
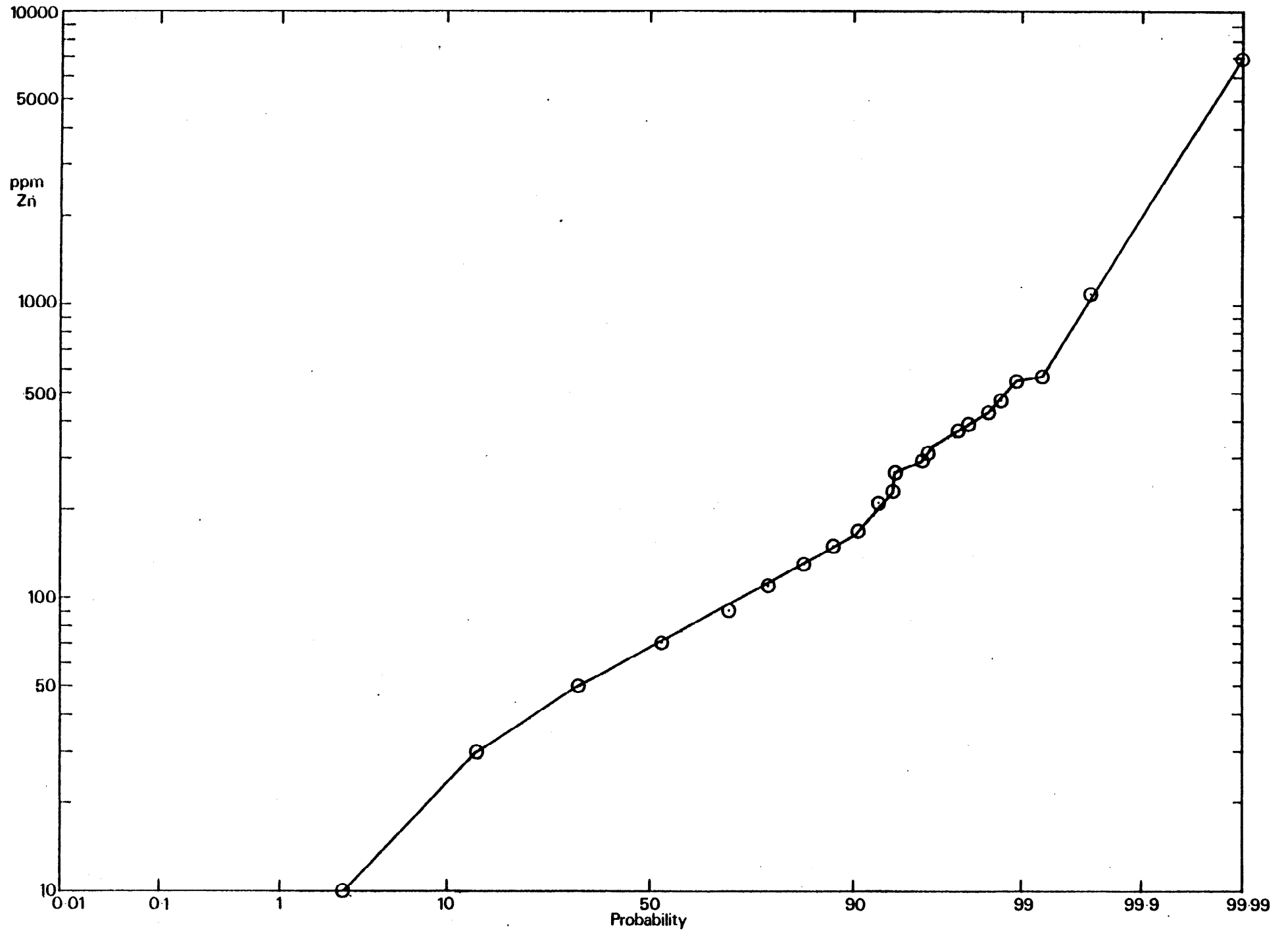
Fig 9 Cumulative frequency plot for zinc (AAS)
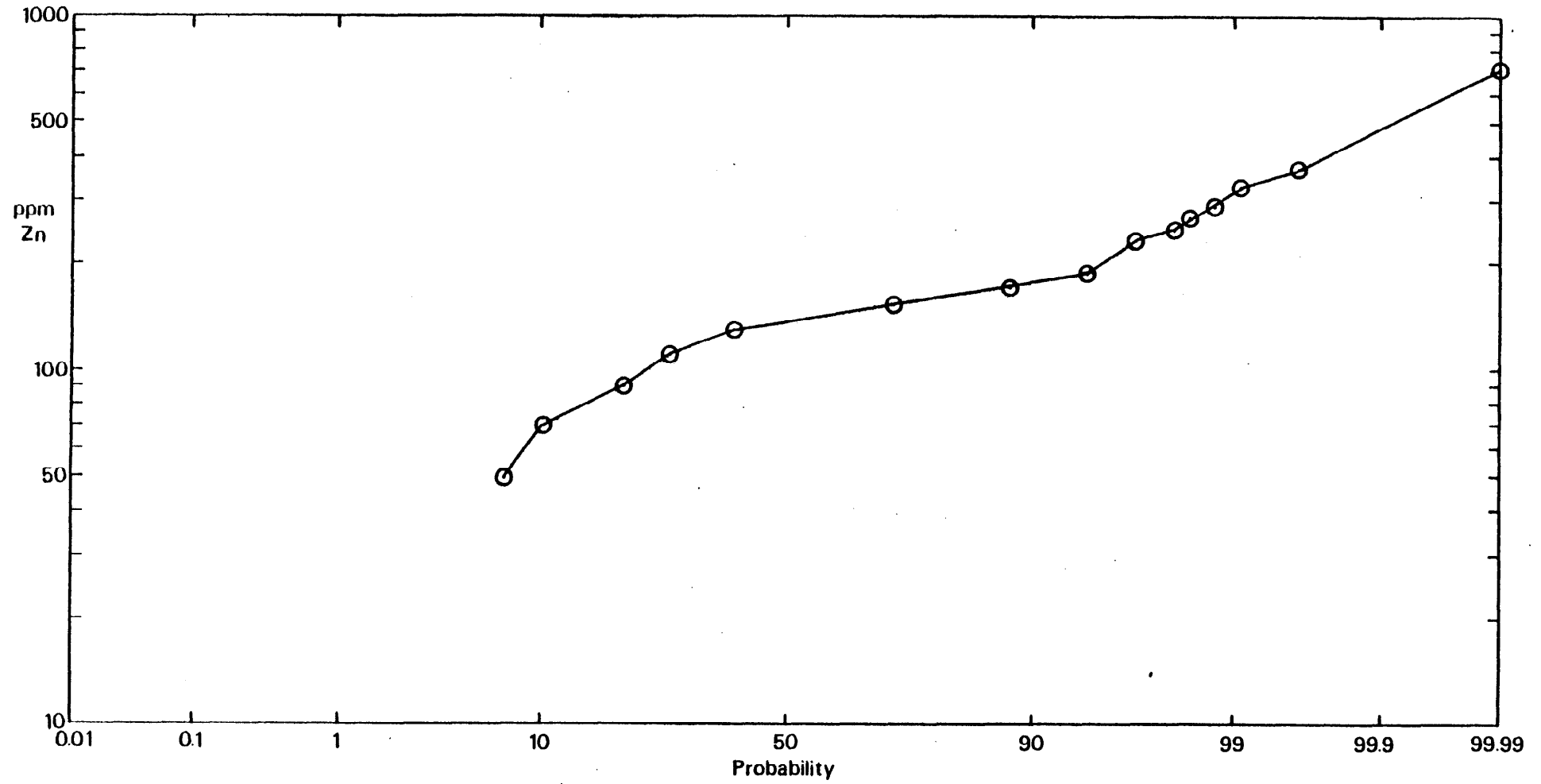
Fig 10 Cumulative frequency plot for zinc (X.R.F.)

14

Fig.11 Contour plot of zinc values in soils

Values shown in ppm.

Topographical contour in feet
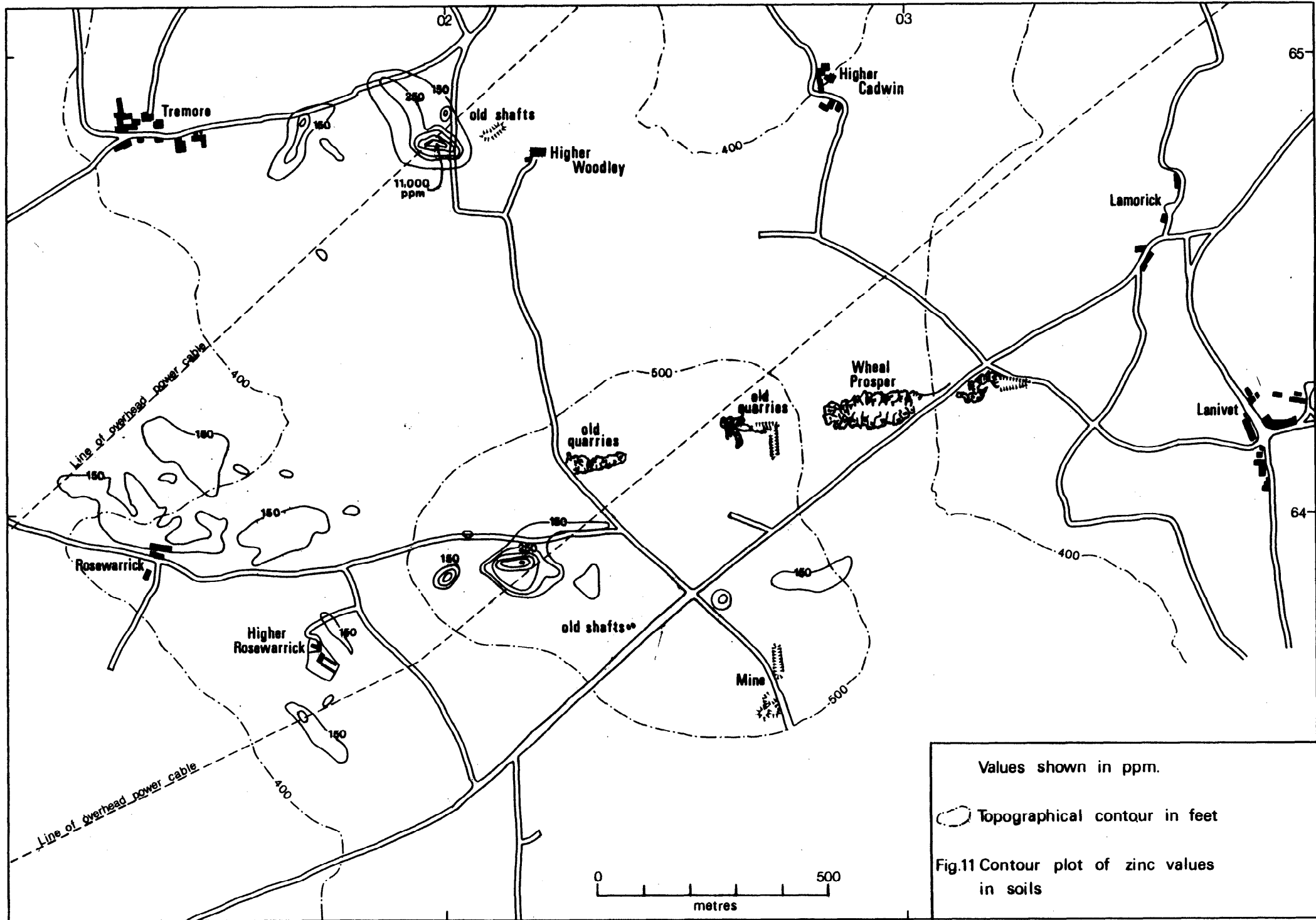
close to an electricity pylon. There seems little doubt that the amplitude of this anomaly is markedly enhanced by contamination but its prolongation northwards and the existence of a further anomaly to the west indicate that there are genuine elevated zinc levels in the local soils. It may be surmised that these originate from the underlying calc-silicate rocks which, in the Consolidated Goldfields boreholes, contained sphalerite distributed as low-grade disseminations and as rare, very narrow, high-grade bands.

Soils from immediately west of the Wheal Prosper quarries were not analysed for zinc and, therefore, the significance of the broad, low amplitude anomalies north of Rosewarrick [014 639] cannot be adequately assessed. It is assumed that they may correlate with the Prosper mineralisation trend; in any event they are too low to be of immediate significance.

In the grouping east of Higher Rosewarrick the central anomaly again lies close to the overhead cable line and may be enhanced by contamination. The individual anomalies closely match those for copper (Figure 8) though there is no consistent ratio between the two metals. There is, again, a suggestion of linearity to the anomaly disposition and parallelism to the Prosper trend.

Tin: Of 642 samples analysed for tin, 416 were determined by optical emission spectrography (OES) and the remainder by XRF. Separately-drawn cumulative frequency plots (Figures 12 and 13) show a marked lack of correlation, the OES levels being distinctly lower than those obtained by XRF. Contoured distribution maps have been prepared therefore for each of the analytical batches, Figure 14 for OES results and Figure 15 for XRF. Each is contoured at 100 ppm intervals but different background levels are used.

The OES plot shows five areas of elevated tin values. In group I the highest tin level occurs close to an electricity pylon, and also near a road, and can reasonably be ascribed mainly to contamination; it is accompanied by very high zinc values. Of the other small anomalies one is adjacent to a road and may be a contamination effect, the others are small and scattered but may reflect sporadic tin minerals (cassiterite or malayaite) disseminated in calc-silicate host rocks. It is significant that this grouping shows no obvious reflection of the Mulberry mineralisation trend.

At II the isolated but high-grade anomaly (max. 825 ppm) almost certainly arises from sampling cassiterite-bearing alluvium which has been extensively turned over and locally strewn around this small valley. The linear anomalies at III and the isolated closure to the west clearly follow the trend of the Prosper mineralisation and indicate a limited westerly extension of that vein zone.

The anomalies at IV and V are both of moderate amplitude, 4 and 5 times background respectively, but do not correlate with known mineralisation trends. The former, however, is located close to the linear copper and zinc anomalies noted previously and accords well with anomalies plotted from the XRF results. Anomaly V is located in a patch of valley alluvium which, though apparently not turned over for tin, probably is cassiterite-bearing.

XRF results are confined to two areas, one north of Rosewarrick and the other south of Wheal Prosper, in both of which there are significant anomalies. In the former grouping the four northerly anomalies all lie within a tract of alluvium which has been extensively turned over for stream tin. The record of tin values of 0.12 to 1.12% suggests that such stretches of "old ground" could repay closer attention from small, mobile alluvial-tin operators. The two major southerly anomalies occur outside the alluvial tract and, though contamination from the spread of streaming waste cannot be ruled out, probably represent a tenuous, patchy extension of the Prosper mineralisation trend.

To the south of Wheal Prosper the results plot as a cluster of tin anomalies but, in part, this distribution is misleading owing to the uneven sampling cover. There is a suggestion of some linearity to the anomalies, according with the copper and zinc results (Figures 8 and 11), but elevated tin values are much wider spread and extend up to 450 m south of the Prosper vein swarm. The scattering of peak values, at levels of 0.11 to 0.33% Sn, is suggestive of sheeted mineralisation comparable to the Mulberry and Prosper bodies.

Tungsten: Only the earlier batch of samples was analysed for tungsten and that by the colorimetric method. Analyses varied from 0 to 50 ppm and the distribution of values is plotted in Figure 16 at contour intervals of 5 ppm above a background level of 20 ppm.

To the west of Higher Woodley three small anomalies close to, but not coincident with, tin and zinc anomalies may represent scattered tungsten mineralisation (scheelite?) in calc-silicate rocks. Two broader anomalies west of the Prosper quarries define continuation of that vein zone and correlate closely with OES tin anomalies (Figure 14). Similarly the small anomaly farther northwest correlates with tin and suggests the presence of wolframite in cassiterite-bearing alluvium.

South of the westernmost Prosper quarry the tungsten anomalies are scattered and of only moderate amplitude but they lie within an area of high tin values and close to major copper anomalies. As with the tin distribution, the scatter of anomalous tungsten results suggests a broad zone of mineralisation to the south of Wheal Prosper.
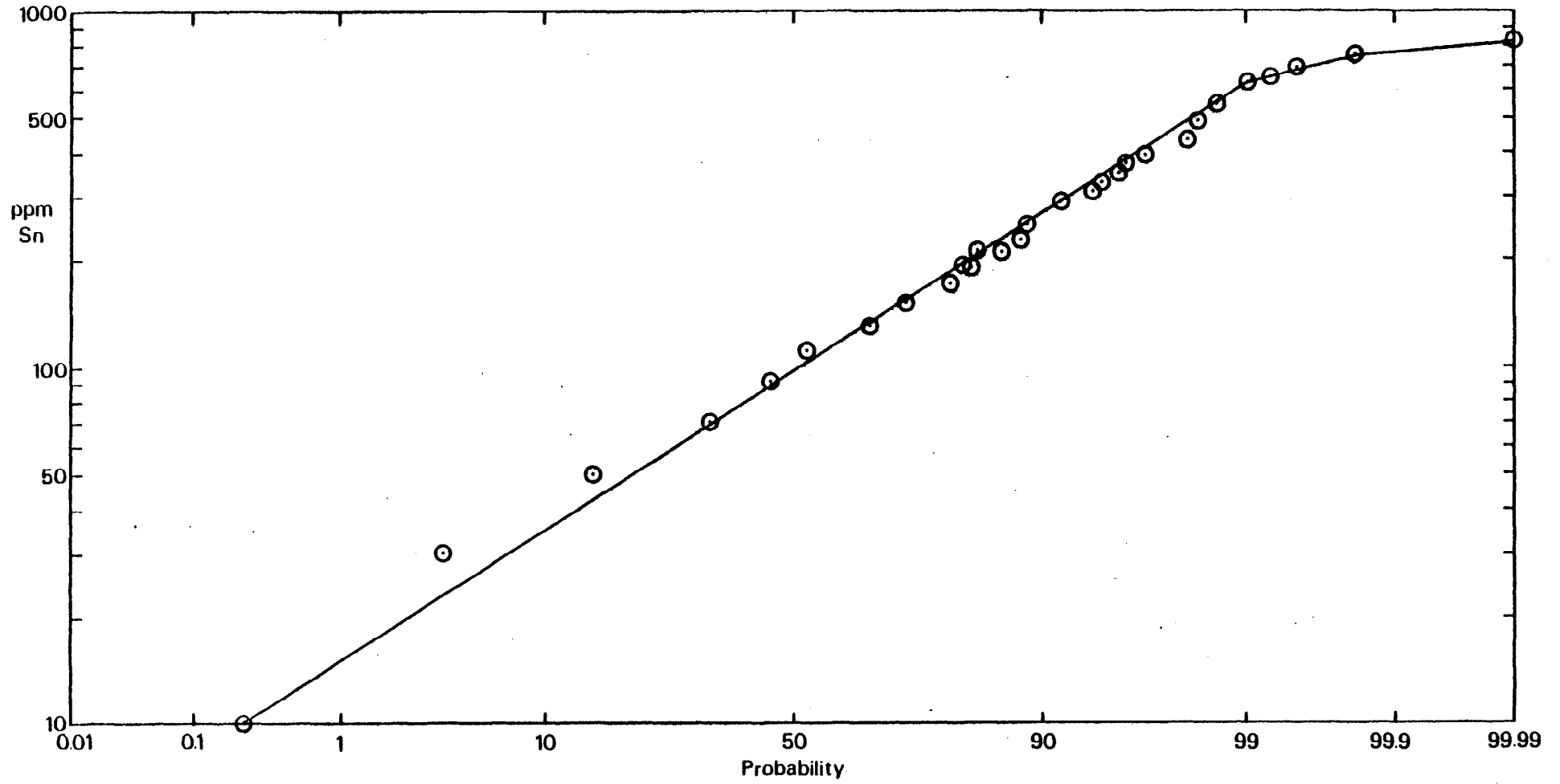
Fig. 12 Cumulative frequency plot for tin (O.E.S.)
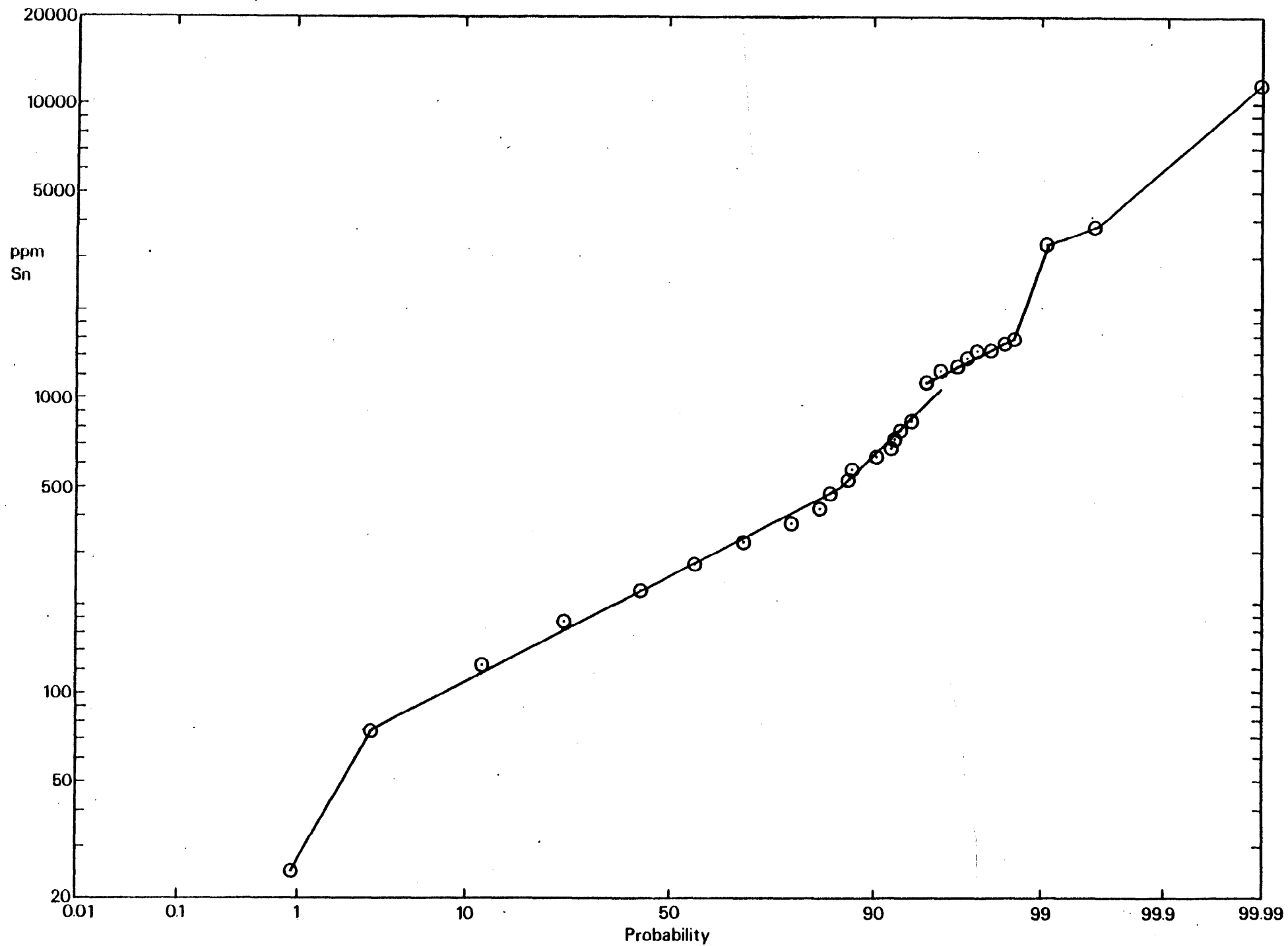
Fig. 13 Cumulative frequency plot for tin (X.R.F.)

18
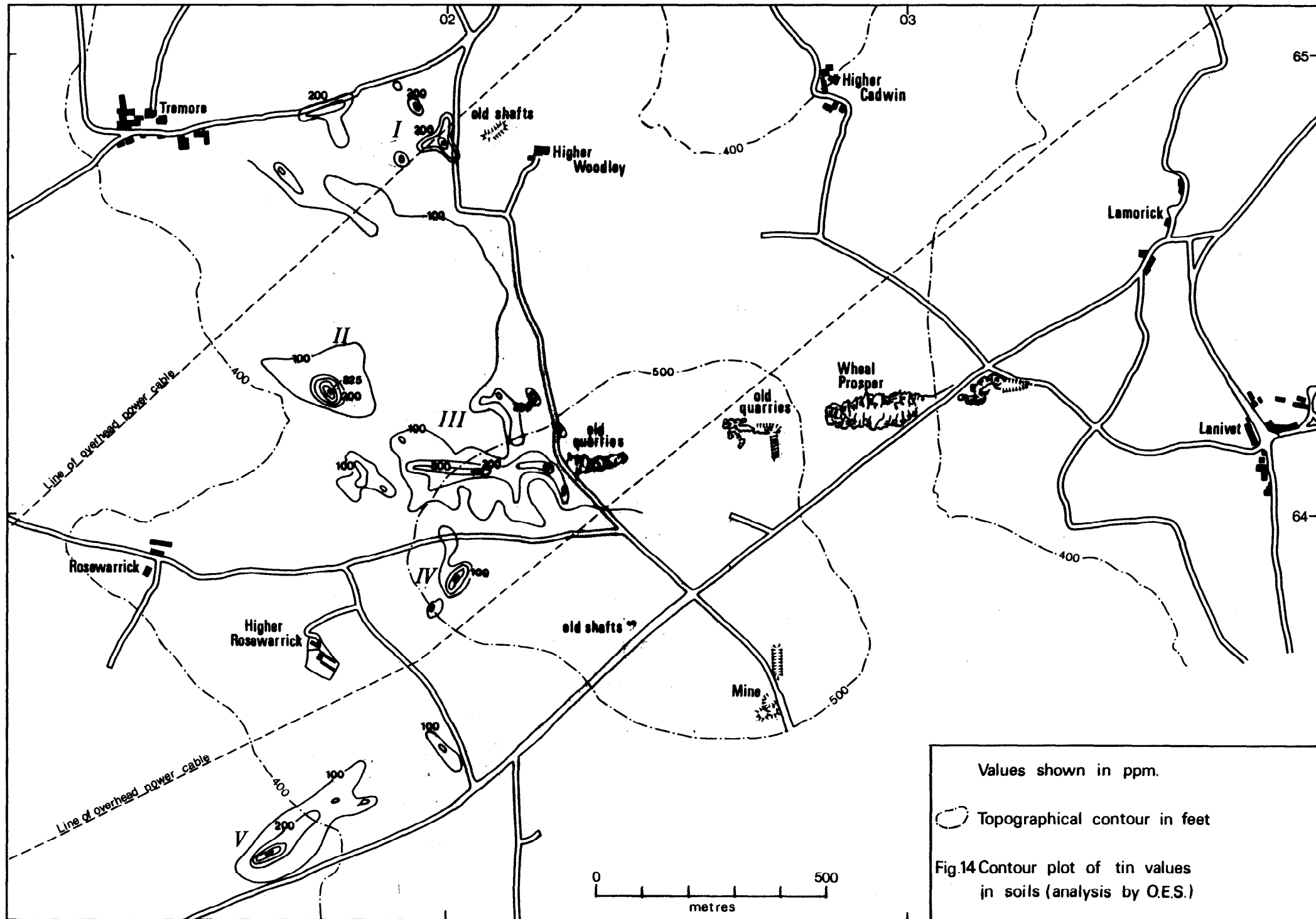
Fig.14 Contour plot of tin values in soils (analysis by O.E.S.)

Values shown in ppm.

Topographical contour in feet

Fig.15 Contour plot of tin values in soils (analysis by X.R.F.)
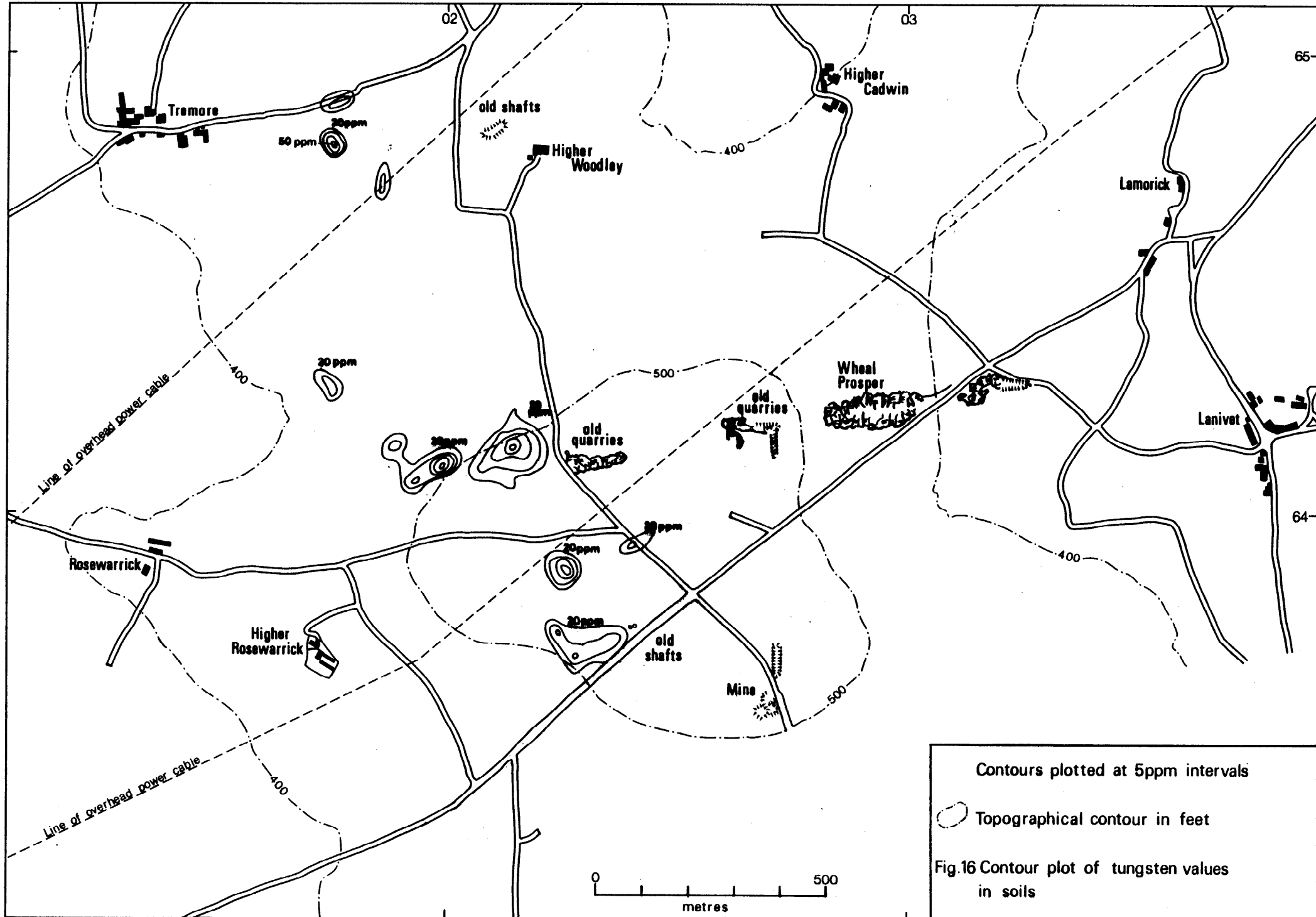
Values shown in ppm.
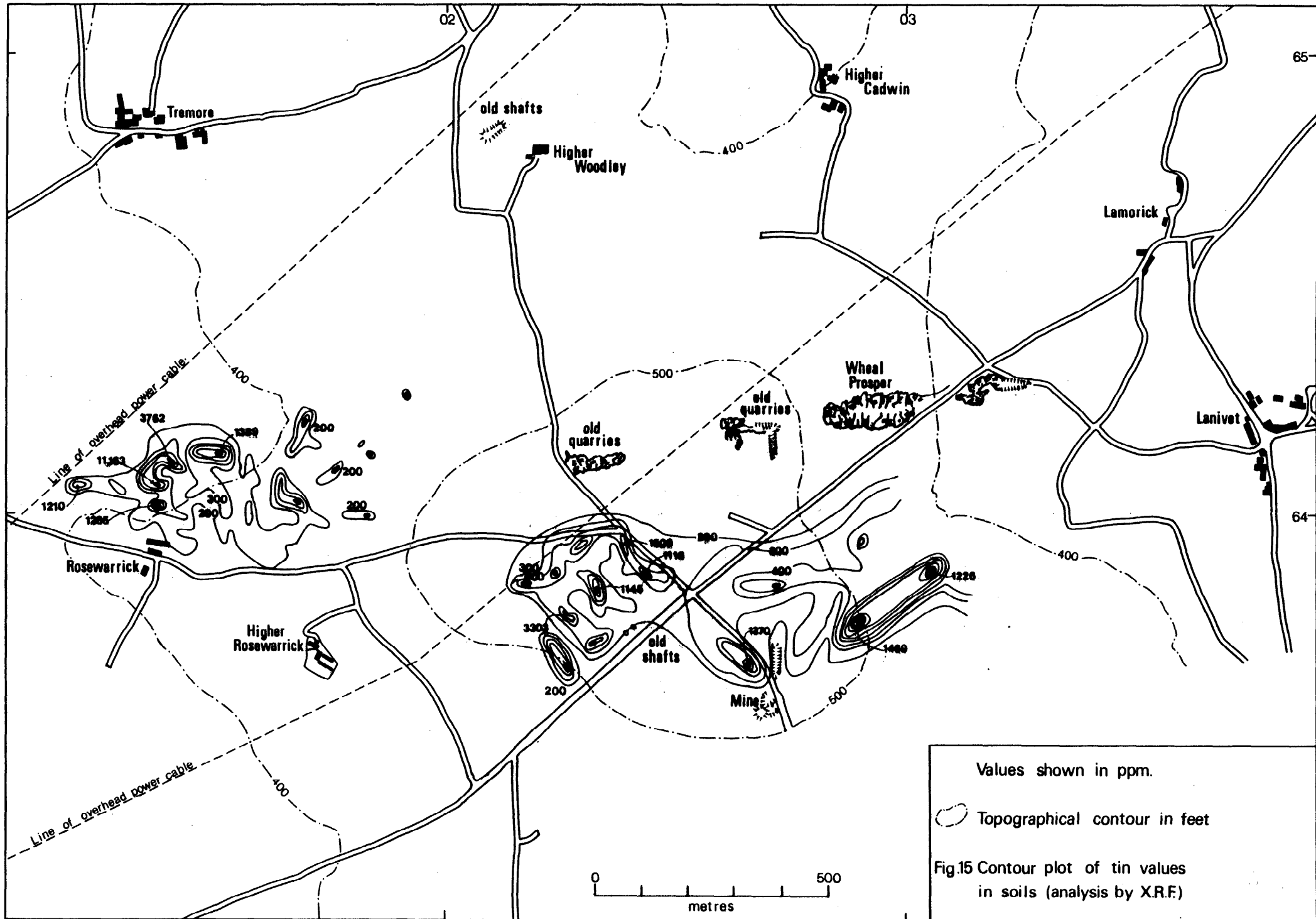
Topographical contour in feet

Contours plotted at 5ppm intervals

Topographical contour in feet

Fig.16 Contour plot of tungsten values in soils

GEOPHYSICAL INVESTIGATIONS

GRAVITY

As part of a wider investigation, covering the northern periphery of the St Austell Granite (Tombs, 1977), gravity measurements were made over the Mulberry-Prosper area at a density of about 10 per square km. Interpretation of the depth to granite was locally confused by the presence of higher density calc-silicate beds but it was apparent that the Mulberry sheeted vein system was not sited over a granite 'high', though the Prosper vein swarm overlies a local rise in the granite roof. Unexpectedly, the gravity surveys revealed no linear features indicative of concealed granite ridges.

VLF-EM SURVEYS

In a broad study of the VLF-EM approach to mineral investigation, Patrick (1978) measured responses over an east-west traverse to the south of the Mulberry openwork and two north—south traverses west of the Prosper quarries. The Mulberry line showed a small (10%) anomaly over the extrapolated extension of the vein swarm zone but interference from power lines to the east affects the readings. Very quiet traces were obtained west of the Prosper quarries with a 90 m zone showing a 5% change in in-phase and quadrature values. This weak anomaly appears to be caused by the same structure which gives a chargeability high in IP surveys and the source, therefore, may be interpreted as only weakly conductive.

INDUCED POLARISATION (IP) SURVEYS

Two IP traverses were measured in 1974, L5 south of the Mulberry openwork and L6 west of the Prosper quarries (Figure 1), and are briefly mentioned by Tombs (1978). Magnetic surveys were also conducted along these traverses but yielded no significant results. Three further lines (L1-L3, Figure 1) were measured in 1976 to the west of the Prosper workings.

Location and orientation of the traverses was limited by land access restrictions and power line interference, preventing extension south-eastwards. A dipole-dipole configuration using 50 m dipoles separated by 300 m (n=6) gave an approximate maximum survey depth of 150 m. The Huntec equipment gave an output of 5 amps, a total cycle time of 8 secs and a duty ratio of unity. For chargeability measurements the delay time (t_d) was 120 millisecs (60 for L5, 6) and the interval sample time (t_p) was 60 millisecs (30 for L5, 6) giving a value integrated between 120 and 1020 millisecs (60 and 510) after the switch off of a 2 secs polarising pulse. An internal and an external 50Hz passive filter were used throughout. Electrical interference was severe in the northern parts of the Prosper lines and at large dipole separations.

Apparent resistivities were generally less than 700 ohm metres and chargeabilities less than 20 millisecs. In L1 (Figure 17), between 150 and 200 m north of origin, there is a zone with chargeabilities above 50 millisecs and apparent resistivities below 200 ohm metres. The source is shallow and probably artificial, but proximity to old mine shafts suggests that a natural source cannot be entirely discounted. No significant anomalies were recorded along L2 (Figure 18). L6 results (Figure 19) are not strictly comparable because of the different instrumental parameters employed. Apparent resistivities increase with depth and towards the south. Maximum chargeability for n=2 occurs roughly due west of the Prosper quarries. Along L3 the apparent resistivity pattern (Figure 20) is similar to that of L6 and chargeabilities are generally low.

A plot of apparent resistivities and chargeabilities for n=2 is shown in Figure 21; chargeabilities along L6 have been multiplied by a factor of 0.5. The axis of the chargeability maximum lies a little to the south of the main Prosper trend but the maximum on L1 correlates closely with the east—west trend of copper and zinc anomalies some 200 m south of the Prosper axis (Figures 8 and 11).

Figure 22 and comparison of the two parts of Figure 21 indicate that chargeability and apparent resistivity vary sympathetically. Changes in apparent resistivity are most likely related to variations in lithology, degree of saturation and pore water conductivity. Amongst lithological variations must be included degrees of quartz veining or mineralisation and it is tempting to envisage the coincidence of high chargeability, high apparent resistivity and anomalous Cu and Zn 200 m south of the Prosper quarries as indicative of a zone of quartz-sulphide veining.

The similarity and regularity of the apparent resistivity pseudosections for L6, L3 and the northern part of L2, when compared with the irregularities in profiles for L1 and the southern part of L2 suggest a major structural break passing through National Grid Reference 020 640 and trending slightly west of north. Such an inferred lineament, either a fault or a late iron lode, could readily explain the abrupt cut-off to the east—west aligned geochemical anomalies east of Higher Rosewarrick.

DRILLING

The western extension of the Prosper vein zone, as indicated by tin-tungsten anomalies, and the broad copper halo to the south of this, were investigated by narrow-diameter diamond drilling using the Institute's JKS 300 rig. Boreholes sites and directions are shown in Figure 2 and details are provided in Table 1. BH1 and its abortive precursor
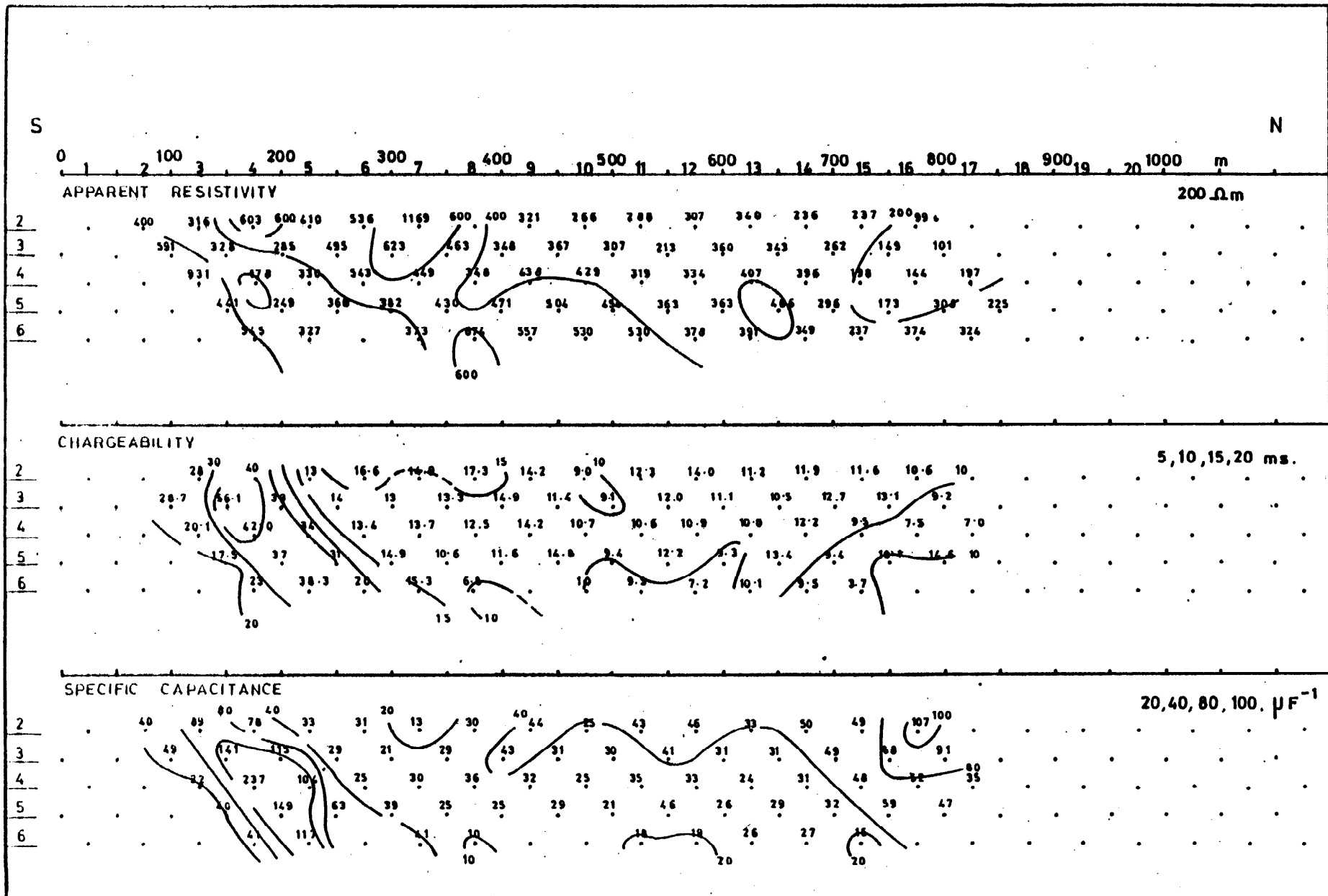
Fig 17. IP pseudosection along traverse L1, Wheal Prosper.

Scale 1:5000

S   0   100   200   300   400   500   600   700 m   N

n   1   2   3   4   5   6   7   8   9   10   11   12   13   14   15

APPARENT RESISTIVITY   200 Ω m

n														
2			419	540 600		400	372	292	214	200 212	162			
3		261	334	472	467	265	366	319	268	364	214	207		
4		219	35	486	310	364	355	406	412	401	308	229	400	
5		320	508	407	547	38	34	581	395	533	315	438		
6		450	493	628	504	379	594	561	510	523	327	433		

0   1   2   3   4   5   6   7   8   9   10   11   12   13   14   15

CHARGEABILITY   5 ms

n														
2		10.5	11.4	14.0	20.0	20	13.7	10	11.9	11.2	10.8			
3		11.3	11.8	15	13.8	11.4	12.4	8.6	8.9	14.2	10.1	10 38		
4		15.5	10.6	16.0	9.7	11.9	9.4	8.0	9.4	12.7	10.4	11.6		
5		14.1	4.9	11.7	12.0	12.6	6.5	11.1	8.3	10.9	11.6	10.8		
6		20.5	11.6	11.9		13.2	6.1		11.0	14.6	10.2	11.5		

1   2   3   4   5   6   7   8   9   10   11   12   13   14   15

SPECIFIC CAPACITANCE   10 μF^{-1}

n														
2		22	27	26	40 45	41	49	56	53	67				
3		43	33	22	30	43	34	27	32	39	47	46		
4		71	7	35	28	33	26	20	23	37	36	48	40	
5		41	23	29	22	37	15	19	21	20	37	24		
6		46	24	19		35	10		22	28	31	26		
				20		30	20							

Fig. 18.   IP pseudosection along traverse L2, Wheal Prosper   Scale 1:5000

S   N

n   0   100   200   300   400   m

APPARENT RESISTIVITY   100 Ω m

2   386   341   325   210   268   264

3   488   360   416   351   327   374   275

4   519   494   467   467   437   398   308

5   681   505   581   456   400

6   664   561   500   300   600

CHARGEABILITY   10 ms

2   25   27   23   23   18   17

3   24   19   30   26   30   18   18

4   16   23   23   29   21

5   19   18   17   21

6   41   23   40   30

SPECIFIC CAPACITANCE μF^{-1}

2   66 75 80 72 100 112 69 66

3   50 53 73 78 91 49 67

4   32 52 50 63 54

5   29 56 30 48 90
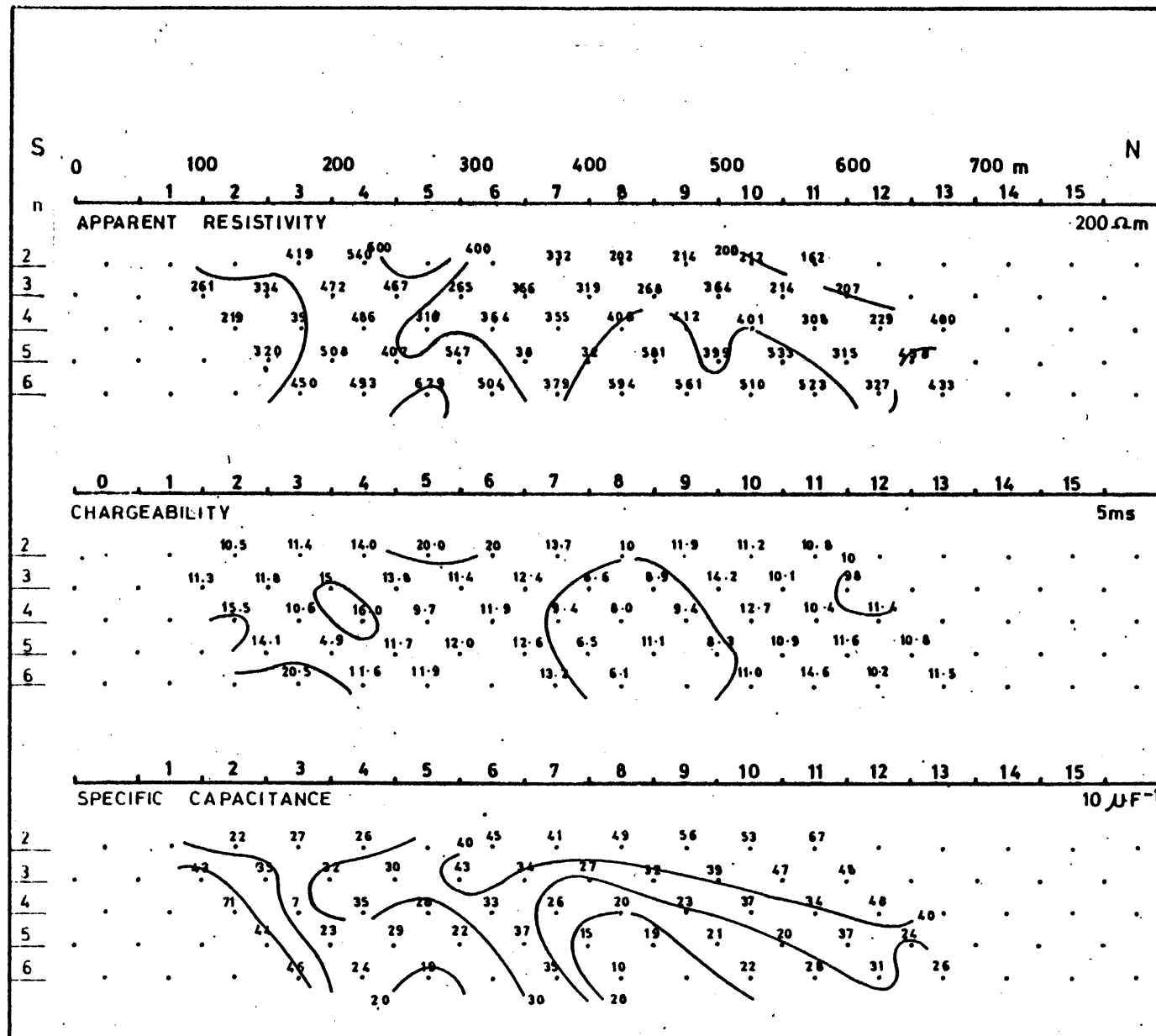
6   50
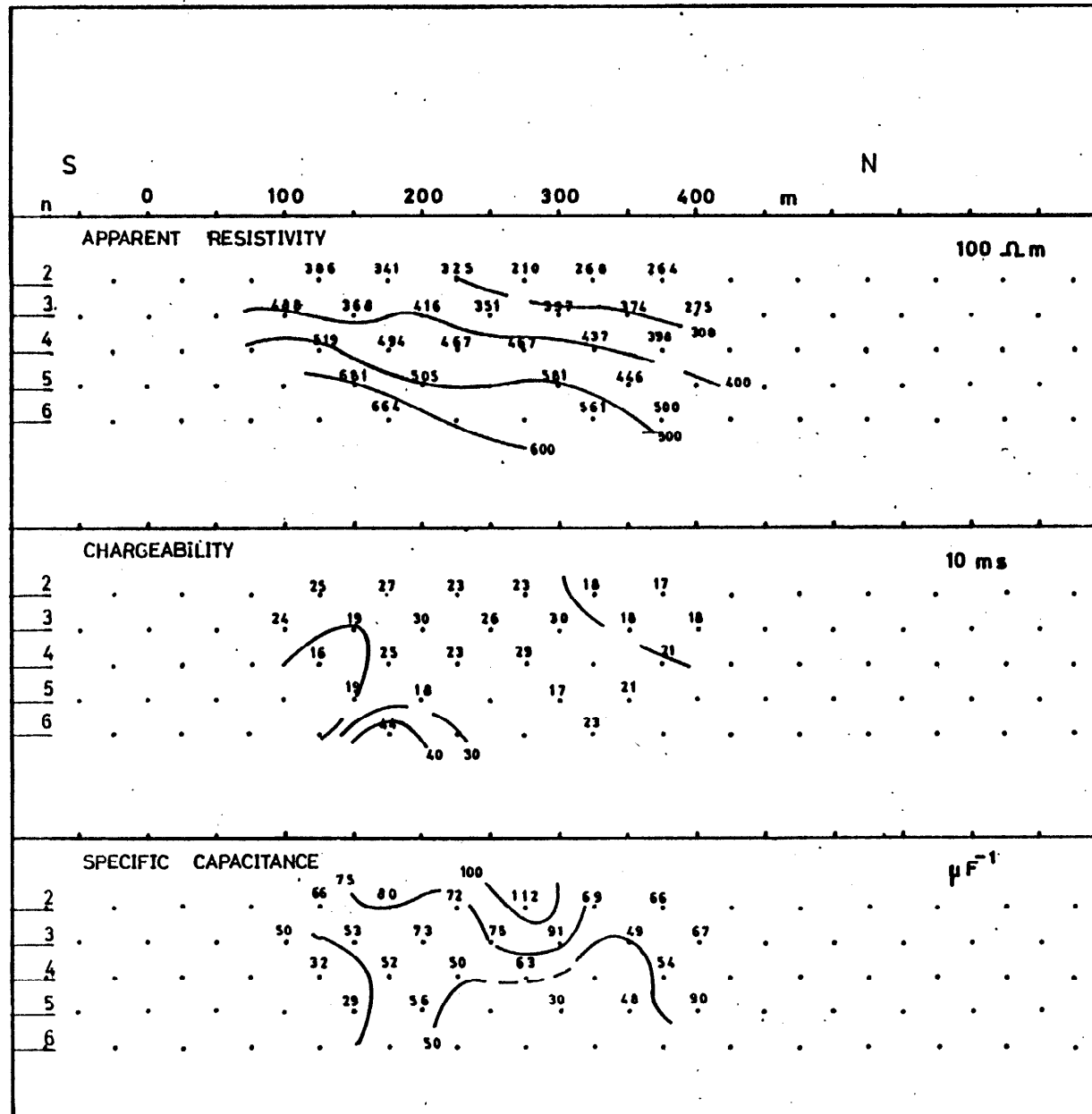
Fig. 19.   I P pseudosection along traverse L 6, Wheal Prosper   Scale 1 : 5000
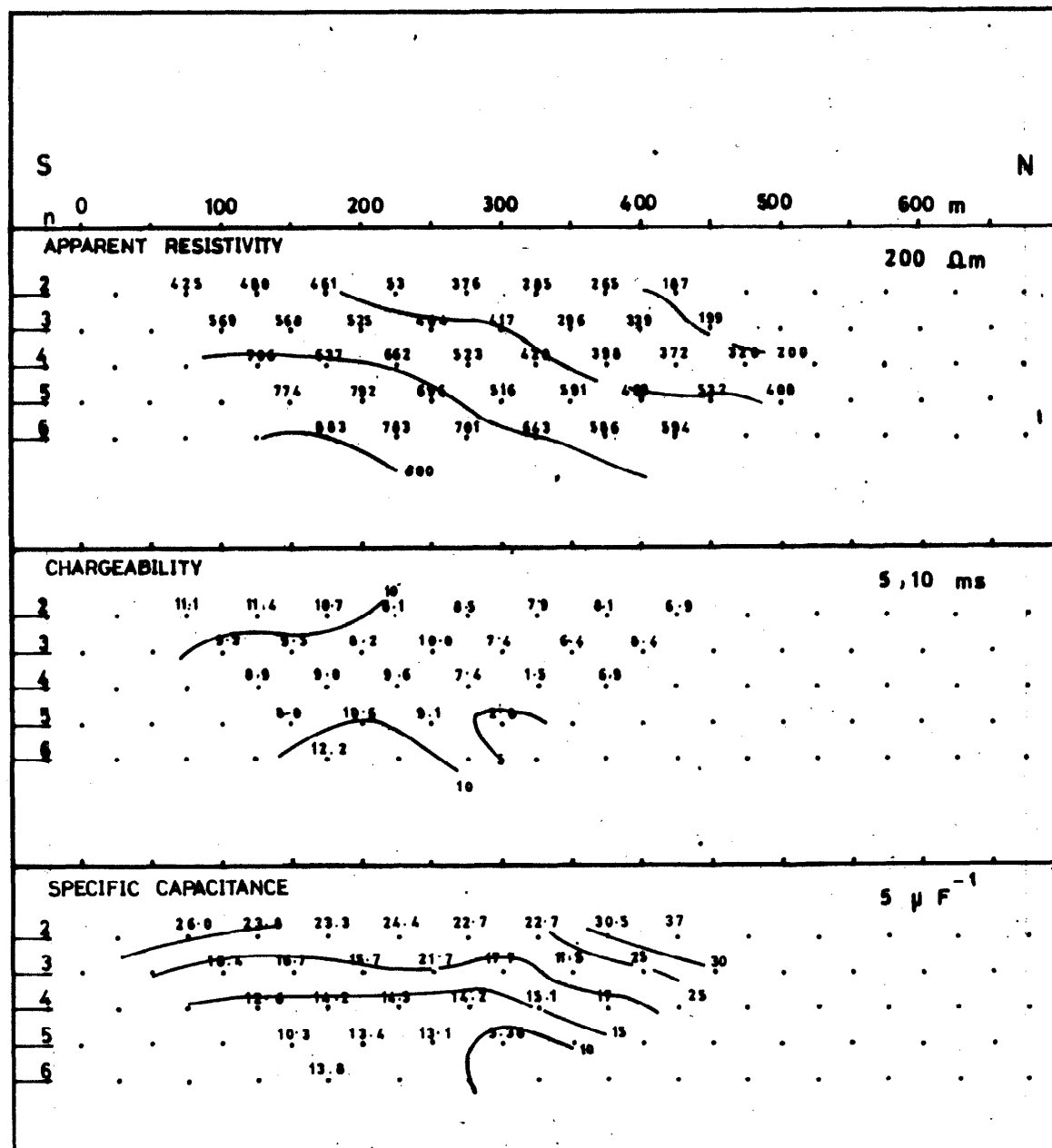
Fig. 20.   IP pseudosection along traverse L3, Wheal Prosper.   Scale   1 : 5000

a. APPARENT RESISTIVITY Ωm
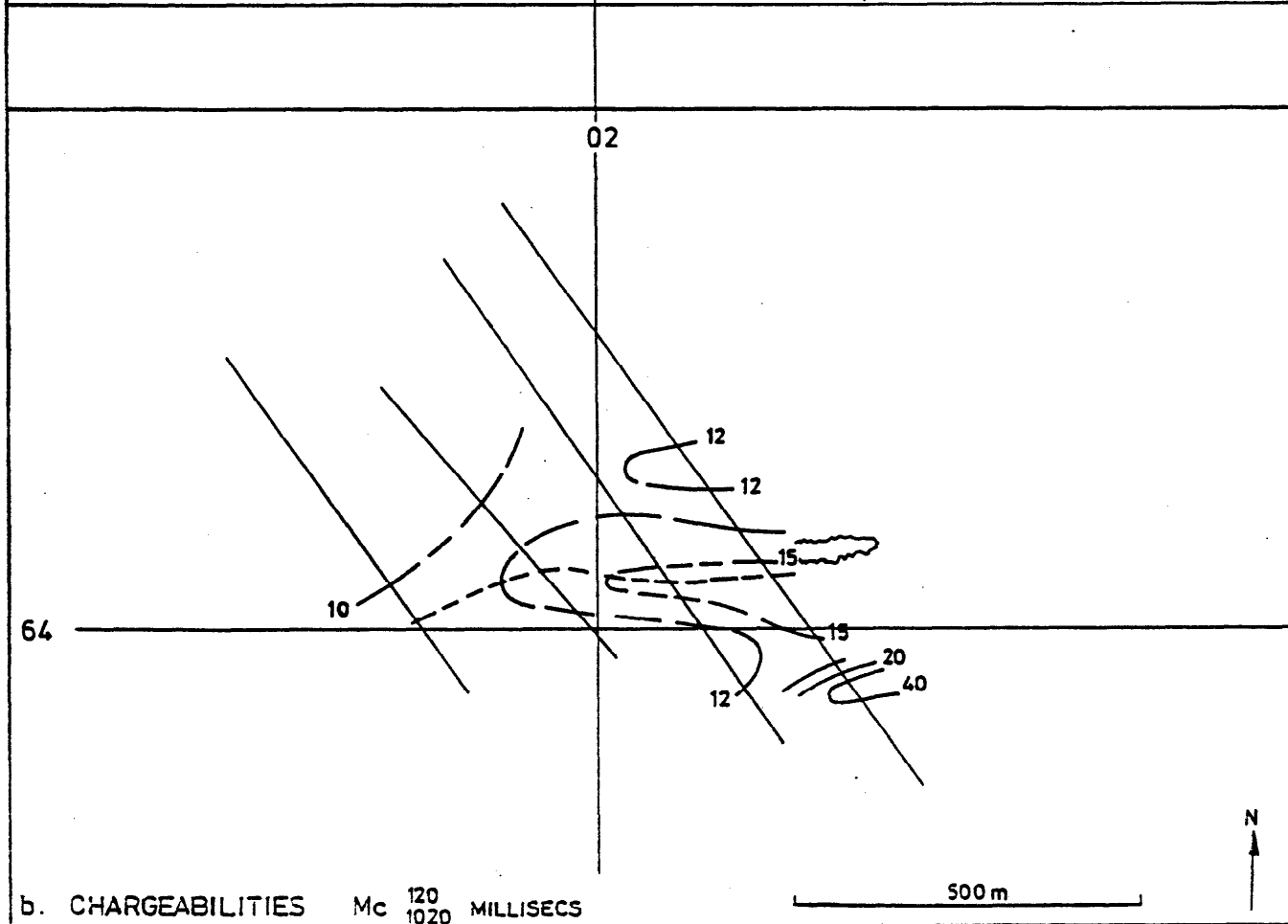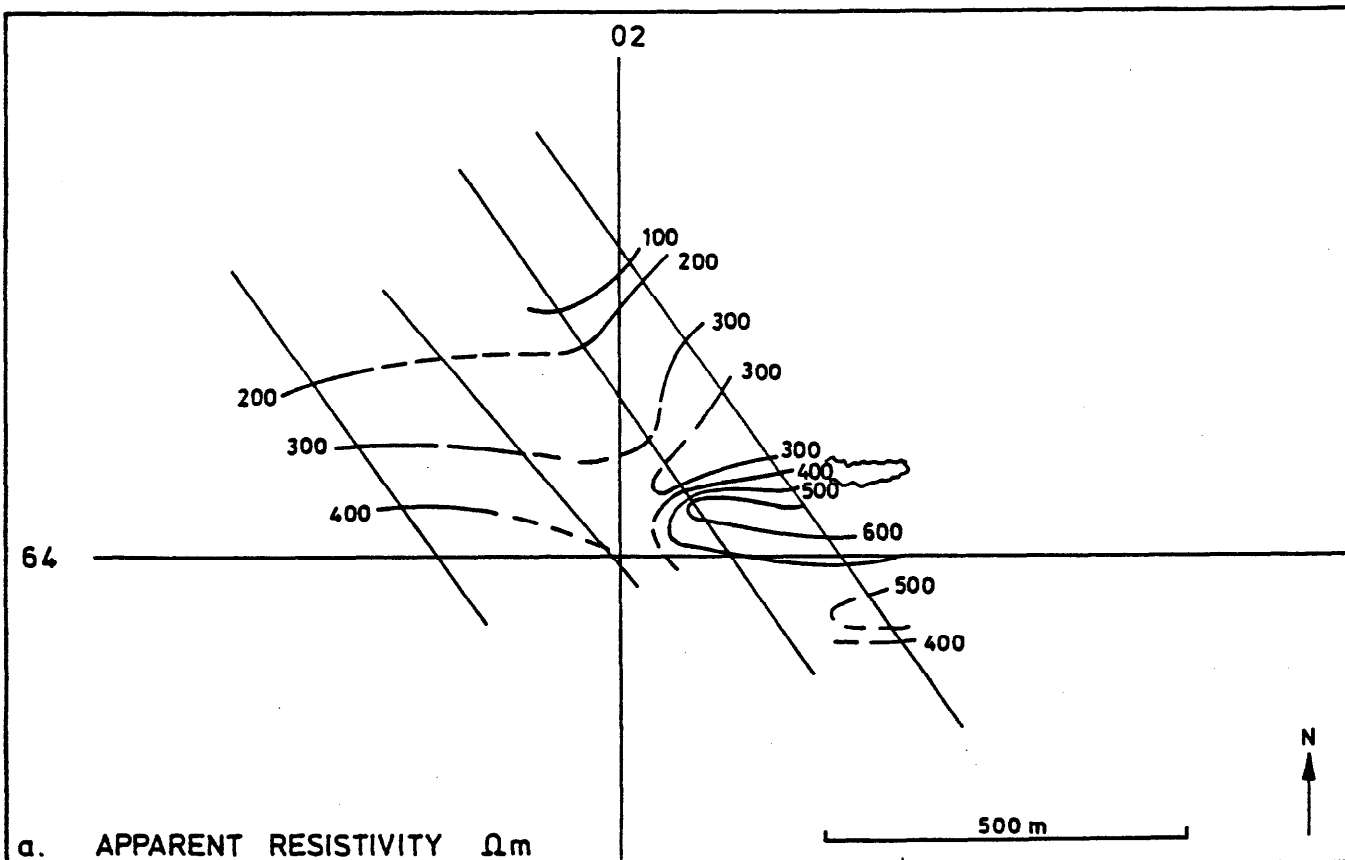
b. CHARGEABILITIES Mc $\frac{120}{1020}$ MILLISECS

FIG.21. APPARENT RESISTIVITY AND CHARGEABILITY PLOTS FOR n = 2, AT WHEAL PROSPER.
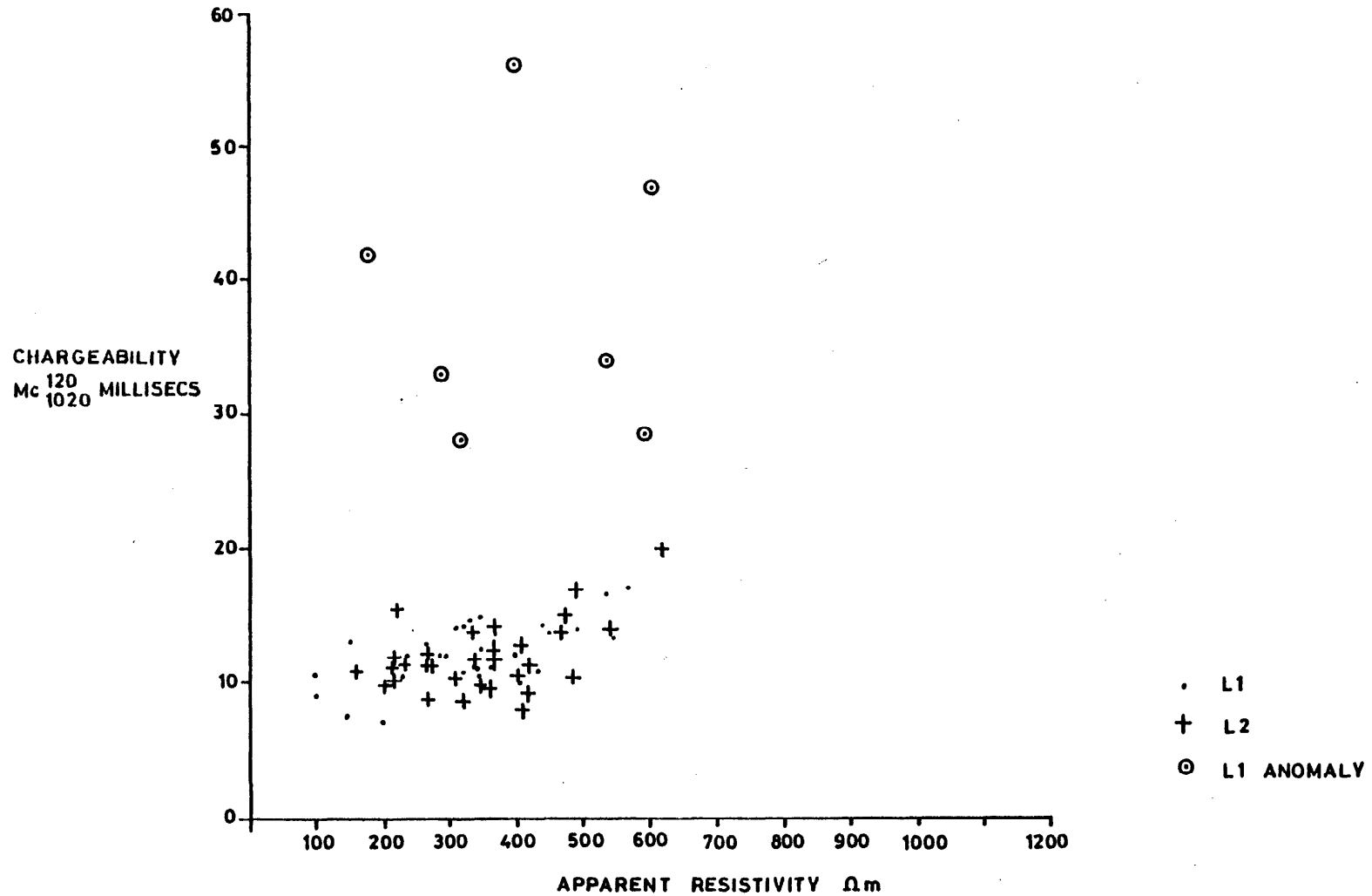
FIG. 22. PLOTS OF APPARENT RESISTIVITY AND CHARGEABILITY FOR
L1, L2 FOR n = 2,3,4 WHEAL PROSPER.

Table 1 Borehole details

BH	Location	Azimuth	Inclination	Completed length
1a	0222 6406	007°M	−60°	41.15 m
1	0221 6407	007°M	−60°	121.92 m
2	0221 6407	186.5°M	−60°	130.45 m
3	0239 6411	186°M	−60°	91.14 m

BH1a examined the Prosper veining, BHs 2 and 3 the copper halo.

Owing to rig availability and farming needs the drilling programme was initiated before XRF analyses from the soil grid had been completed and before the inferred mineralisation 200 m south of the Prosper workings had been recognised; and as a result the latter was not drilled.

CORE GEOLOGY

All four boreholes were located within the outcrop of the Meadfoot Beds and penetrated a succession of grey slates, sandy slates and occasional calc-silicate layers. Colour variation is common and emphasises the bedding and occasional zones of pronounced folding. Near to surface the rocks are highly weathered and widely iron stained or locally bleached; but below about 45 m they are relatively unaltered and compact though well jointed throughout. In the calc-silicate bands alteration persists to greater depths and is believed to be caused by the passage of hydrothermal fluids through this more porous, granular rock type.

Joint surfaces in the slates are commonly coated by iron and manganese oxides, by thin films of tourmaline and white mica developed in radiate clusters, and by pyrite either as films or small discrete crystals. Calcite and hematite coat the fracture surfaces in calc-silicate bands and are, rarely, accompanied by axinite.

Quartz veining, though common, tends to be developed irregularly throughout the succession with alternating zones of minor and intense veining. Most veins are narrow, rarely wider than 10 mm, and contain varying amounts of tourmaline, usually near or along their margins. Metallic ore minerals are generally scattered through the veinlets as small spots or crystals but pyrite is occasionally clustered into narrow pods at the veinlet walls. Pyrite and cassiterite are the commonest ores and are seen in all four boreholes, though most abundantly in BH 1. Chalcopyrite and arsenopyrite are often associated with cassiterite, especially in BH 1, but both occur individually with the arseno-pyrite rarely forming minute veinlets. Some chalcopyrite is altered to green secondary copper minerals but scorodite, the alteration product of arsenopyrite, was not observed although it has been reported from the Mulberry openwork.

Detailed geological logs of the boreholes are given in Appendix I.

CORE GEOCHEMISTRY

A total of 42 samples from the cores were crushed for XRF determination of Sn, W, Cu, Pb, Zn, As, Ba, Sr, Zr, Mo, U and Ce. Sampling details are listed in Appendix II and the analytical results shown diagramatically in Figures 23 to 26; lead values are not included because of XRF interference from tin.

The most significant feature in BH 1a (Figure 23) is the geochemical signature of the calc-silicate horizons, with elevated levels of Cu, Zn, Zr and Ce. Unfortunately, the upper horizon was not penetrated by BH 1 and the lower horizon was not recognised or sampled. A similar Zr-Ce signature is not found in the calc-silicate of BH 2 (Figure 25), suggesting variations either of original composition or of metasomatic alteration. In this respect, the high Zr and Ce levels may be adduced to indicate an original tuffaceous or volcanic composition for the BH 1a calc-silicate beds. Although chalco-pyrite and sphalerite are commonly disseminated through the calc-silicate bands, as was observed in the Consolidated Goldfields boreholes, in BH 1a these layers are highly altered and Cu and Zn are probably held mainly in the manganese and iron oxides which pervasively stain the rocks. At the base of the lower calc-silicate band there are low but significant contents of Sn and W; but no tin or tungsten mineralisation was noted in the core. The elevated copper value at the base of the borehole correlates with observed secondary copper minerals but no ores were seen to account for the arsenic content; this, also, may be held in the iron oxides.

Of 17 samples analysed from BH 1, 13 exhibit tin contents of 100–900 ppm; even in the richest of these there is no visible cassiterite which, if present, must be fine grained and disseminated in the wall rock of quartz veinlets. The other 4 samples were taken from zones of significant quartz-cassiterite veining. From the distribution of tin values in this, the hole richest in visible cassiterite, it can be recognised that the ore grade is distinctly subeconomic. Tungsten levels are generally less than 50 ppm. Of the exceptions two, both low grade, are associated with the highest tin values, indicative of traces of wolframite associated with the cassiterite in quartz veining. A third, the highest content at 1371 ppm, occurs in a quartz-tourmaline vein some 20 mm wide and is accompanied by 3000 ppm Sn and 3400 ppm As. Re-examination of this veinlet under binocular power revealed fine-grained wolframite, cassiterite and arsenopyrite interstitial to the tourmaline. The fourth exception, at 255 ppm, is associated with very high arsenic (6103 ppm) and presumably represents traces of wolframite accompanying arsenopyrite in quartz veining.

All the high copper and arsenic values correlate well with recorded visible mineralisation but, significantly, neither element is consistently associated with either tin or tungsten. Of the remaining elements determined, none shows a uniform
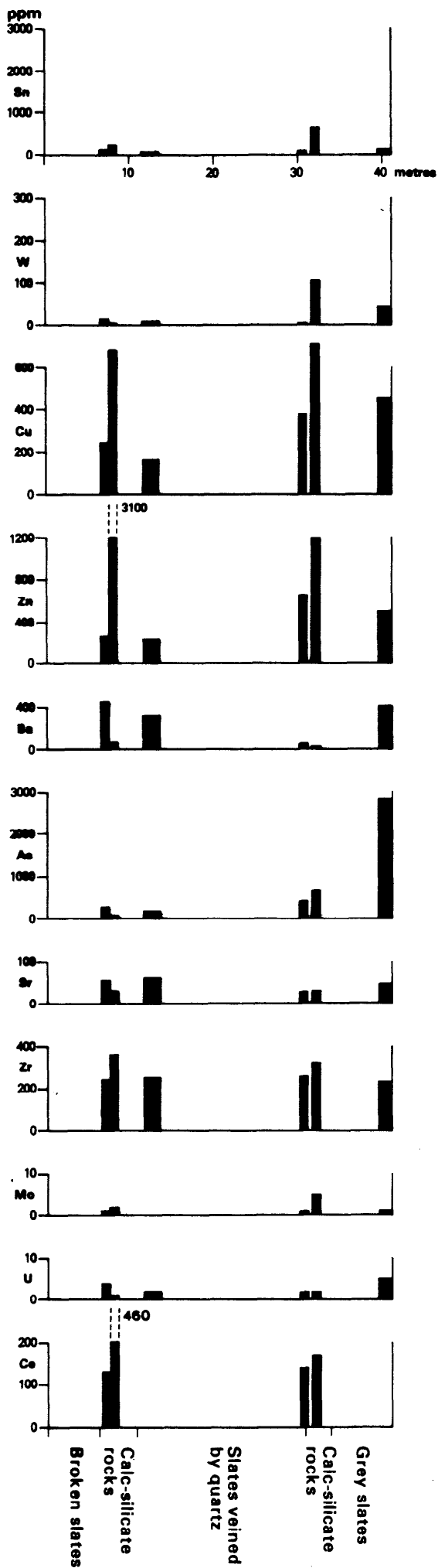
Fig. 23 Core geochemistry, Prosper BH1a

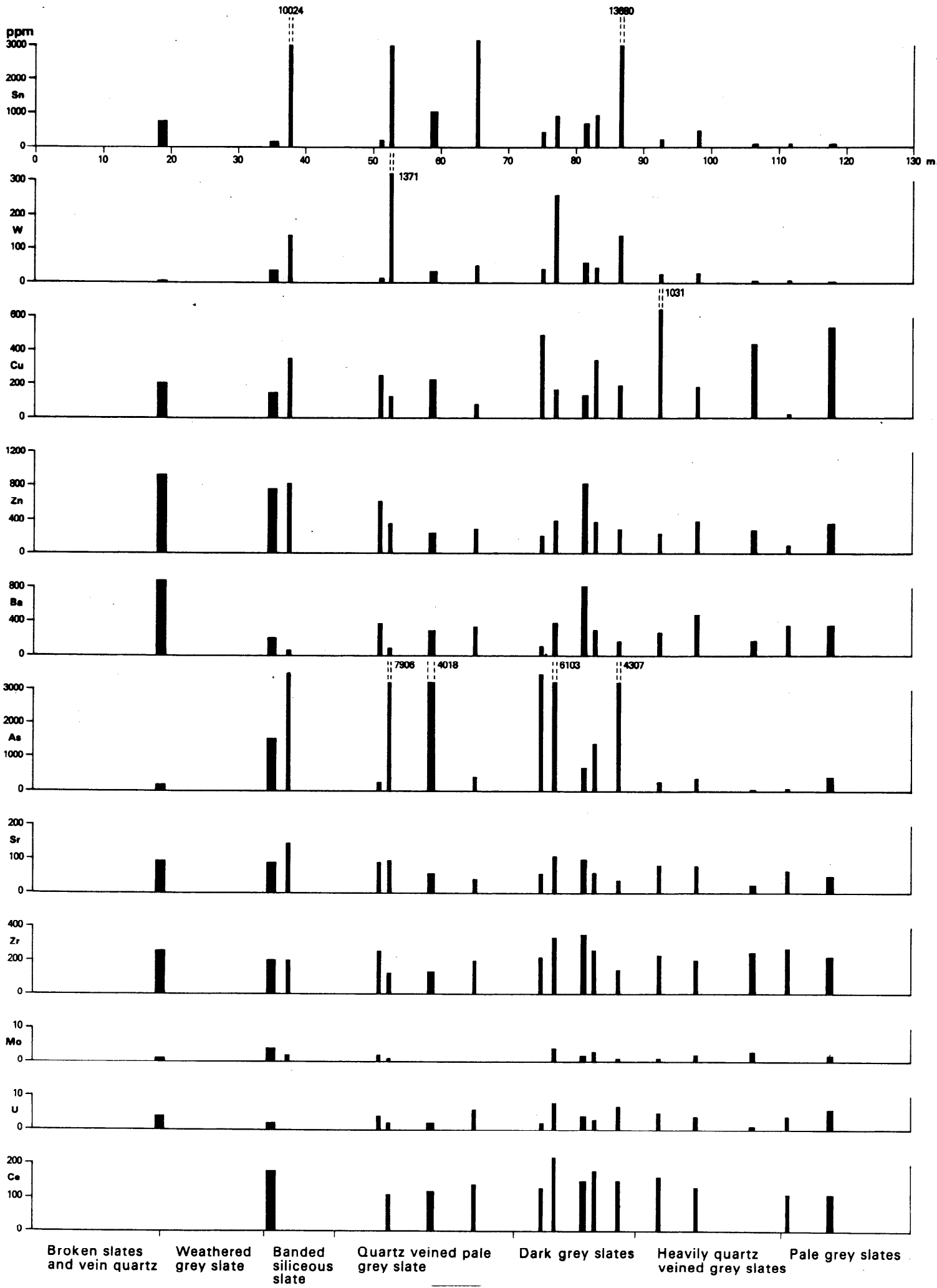Fig.24 Core geochemistry, Prosper BH1
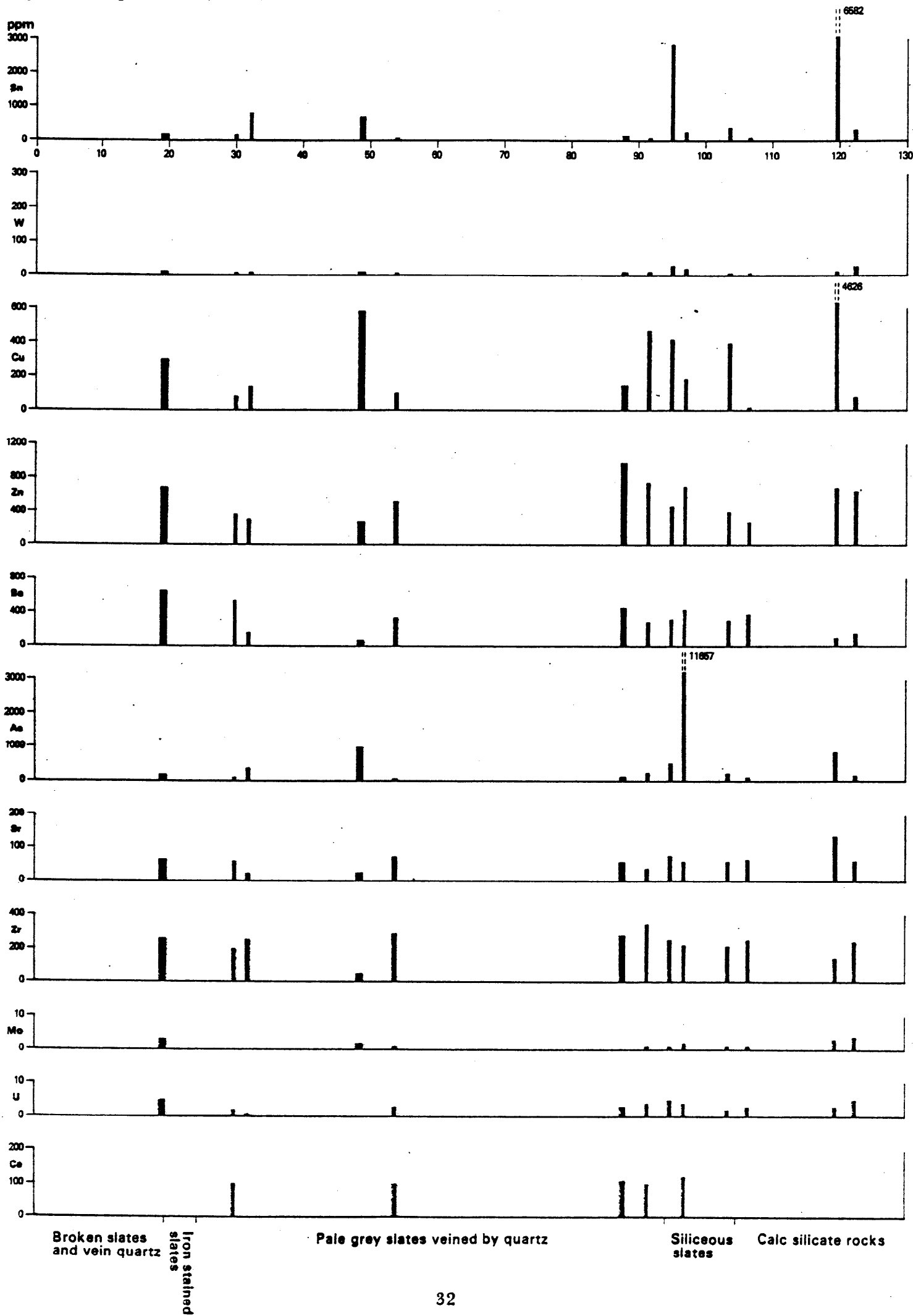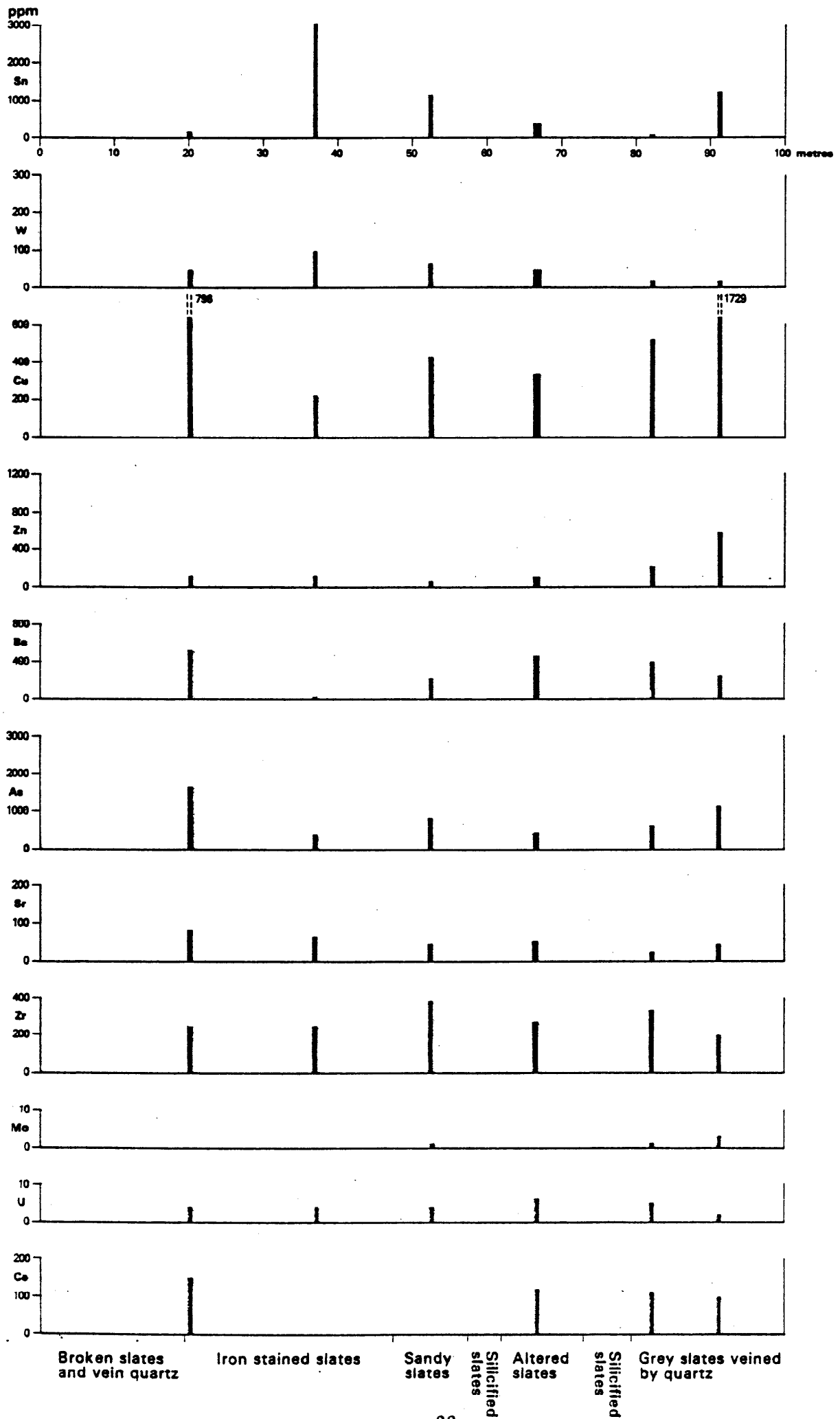
Fig. 25 Core geochemistry , Prosper BH 2

32

Fig. 26 Core geochemistry , Prosper BH 3

33

pattern of correlation with the main ore metals or with the degree of quartz veining.

Only 2 of the 13 samples from BH 2 show high tin contents and none contains more than 30 ppm W. Values of 2900 ppm Sn and 420 ppm Cu were determined from 94.50 to 94.80 m in slate veined by quartz carrying cassiterite, pyrite and chalcopyrite. Higher values still, 6582 ppm Sn and 4626 ppm Cu, were obtained from an axinitic skarn-like band within calc-silicate rocks at about 199.5 m. Brown cassiterite was noted in this band but no copper minerals were apparent to the naked eye. The only arsenic peak, a remarkable 1.2% As, was recorded on a greiseny quartz-arsenopyrite veinlet at 96.93 m; this vein carries only low copper and zinc contents and virtually no tin.

In BH 3 there is only one tin peak, of 3100 ppm, in altered iron-stained slates cut by fine tourmaline veinlets. No cassiterite was seen in the core but presumably this mineral is finely disseminated and associated with the tourmaline veining. A small copper peak at about 20 m depth also occurs in iron-stained slates and here the copper may be in a redistributed secondary phase. The other copper peak, near the bottom of the borehole, derives from green secondary minerals occurring within quartz veining. None of the other ore metals are present in significant quantity.

Despite the irregularity of sampling, a visual scan of Figures 23–26 provides a meaningful correlation with the surface geochemistry. In BH 1 a cluster of tin values over 800 ppm stretches from 37.5 to 87.0 m and represents the westward extension of the Prosper vein zone. By comparison, high tin values in BHs 2 and 3 are widely separated, reflecting isolated small mineralised structures. Copper levels in BHs 2 and 3 attain higher levels than in BH 1 and more of the samples are significantly mineralised; taking into account the sampling lengths the average copper content of BH 1 samples is only half that of BHs 2 and 3 samples. As has been indicated, some of this copper is ascribable to the presence of chalcopyrite and some to green secondary copper minerals but a portion probably reflects elemental copper scavenged and retained by secondary iron oxides, which line many joints and locally pervade the strata.

CONCLUSIONS

Soil geochemistry identifies no continuity of mineralisation between the Mulberry and Criggan vein swarms but outlines an area of particular interest for tin, tungsten and copper in the area west and south of the Prosper quarries. Former exploration had traced the Mulberry mineralisation southwards into the calc-silicate belt but the present survey cannot extend this farther south with any certainty. Scattered anomalies west of Higher Woodley may reflect local mineralisation on the Mulberry trend but equally may represent con-

tamination deriving from the installation of overhead power lines.

The westward continuation of the Prosper mineralisation is clearly defined by soil geochemistry, and drilling proved the existence of tin-bearing veinlets, though insufficient in number or proximity to constitute a workable deposit. A broad geochemical copper anomaly fringing the tin anomaly, and particularly well developed along its southern flank, is explained partly by primary chalcopyrite in quartz veining, partly by secondary copper minerals but probably mainly by redistributed copper adsorbed on iron oxides and clay minerals.

Probably the most promising area is that to the south of the Prosper quarries where geochemistry suggests the possiblity of a previously unrecognised zone of mineralisation sub-parallel to the Prosper veins and some 200 m from them. A less clearly defined IP anomaly over this zone may indicate some depth continuity to mineralised quartz veining. Unfortunately this zone was not fully recognised prior to drilling and, therefore, has not been tested. The geochemical anomalies extend over a width of almost 300 m and a strike length of 1100 m, though the eastern limit of the anomalies has not been defined with certainty. This zone would seem to be a prime target for future drilling.

Spectacular tin anomalies north of Rosewarrick probably reflect the spread of tin-bearing alluvium during earlier tin-streaming activities. Some of the analyses suggest that rich ore (better than 2 lbs/cu. yd.) still remains in these deposits and that the relatively small tonnages available could profitably augment any in-situ tin reserves.

REFERENCES

COLLINS, J.H. 1912. Observations on the West of England mining region. Trans. R. Geol. Soc. Corn., Vol. 14.

DINES, H.G. 1956. The metalliferous mining region of south-west England. Mem. Geol. Surv. G.B., 2 vols.

GROVES, A.W. 1941. Report on the iron ores of Great Britain to the Home Ores Department, Ministry of Supply [unpublished].

HOSKING, K.F.G. 1969. The nature of the primary tin ores of the south-west of England. in *A second technical conference on tin, Bangkok* (Ed. W. Fox), Vol. 3, pp. 1157–1244.

JENKIN, A.K. HAMILTON 1964a. Mines and miners of Cornwall. Vol. 9 — Padstow, St Columb and Bodmin. *Bracknell; Town and Country Press.*

— 1964b. Mines and miners of Cornwall. Vol. 8 — Truro to the clay district. *Bracknell: Town and Country Press.*

PATRICK, D.J. 1978. VLF-EM studies in areas of known mineralisation in Britain. *Rep. Applied Geophysics Unit, Inst. Geol. Sci.,* [unpublished].

TOMBS, J.M.C. 1977. A study of the space form of the Cornubian granite batholith and its application to detailed gravity surveys in Cornwall. *Miner. Reconnaissance Programme Rep. Inst. Geol. Sci.,* No. 11.

— 1978. Mineral investigations near Bodmin, Cornwall. Part 1 — Airborne and ground geophysical surveys. *Miner. Reconnaissance Programme Rep. Inst. Geol. Sci.,* No. 25.

USSHER, W.A.E., BARROW, G. and MACALISTER, D.A. 1909. The geology of the country around Bodmin and St Austell (Sheet 347). *Mem. Geol. Surv.*

Borehole 1a.

Classification	*Description*	*Thickness (m)*	*Depth (m)*
OVERBURDEN	Highly weathered and bleached slate. Iron staining near base	6.71	6.71
MEADFOOT BEDS Calc-silicate horizon	Highly decomposed calc-silicate band. Greenish-grey in colour with much iron staining on joint faces. Talcose coatings on joint faces at 11.28 m	4.87	11.58
Altered slate	Slates varying in colour from white to red. Quartz fragments seen at 11.89, 12.19 and 14.94 m. Small fissures cutting the slates at 14.48 m are filled with tourmaline and iron oxides	3.36	14.94
Grey slate	Folded grey slates with frequent iron oxide staining. Tourmaline bands follow the bedding from 14.94 to 17.98 m, but at 19.51 m tourmaline and quartz fill a fracture parallel to core axis. White clay band at 26.82 m	16.46	31.40
Calc-silicate horizon	Compact grey-green rock with patches altered to black clay. Iron and manganese oxide staining on joint surfaces	6.40	37.80
Grey slate	Friable grey slate, indurated in part with iron staining and green copper secondaries at 40.54 m. Bedding at 20° to core axis.	3.35	41.15

End of borehole

Borehole 1

OVERBURDEN	Broken fragments of quartz and slate	18.28	18.28
MEADFOOT BEDS Grey Slate	Friable and highly weathered slates with iron staining on broken surfaces. Banding of the slates varies in colour from brown to grey. Tourmaline is present as veinlets associated with quartz at 19.50, 20.73, 22.86 and 26.21 – 26.52 m, the last of these veins being 6.35 cm in width and carrying some iron staining. Small pyrite crystals on broken fragments at 28.65 m. Quartz veining evident at 31.69 – 32.00, 33.22 and 33.53 m, usually less than 3.0 mm in width and some at 70°, others at 15° to core axis	15.86	34.14

Borehole 1 continued

Classification	Description	Thickness (m)	Depth (m)
Banded siliceous slate Sn Sn Cu As	Dark grey slates with occasional quartz veining. Siliceous banding along bedding. Quartz veins sub-parallel to core axis at 34.75 m where tin is indicated by PIF. Tourmaline is associated with these quartz veins at 35.36 and 35.97 m. Quartz veins of 6.3, 9.5 and 3.0 mm width occur at 36.58, 37.64 and 38.10 m respectively with tin indicated by PIF at 37.64 and 38.10 m and pale green copper secondaries in all three veins. At 37.64 m tourmaline crystals associated with poorly formed crystals of arsenopyrite line the vein. The slate is softer from 40.23 to 40.84 m and quartz veins occur at 41.15, 42.06, 42.98 and 44.04 m	11.27	45.41
Altered slate	Rotten, grey brown slate with clay bands and iron staining on broken faces	3.36	48.77
Grey slate Cu Sn Sn	Pale grey slates, broken in part with iron staining on fracture faces. Quartz veins at 48.92, 56.36, 70.04, 70.40, 71.93 and 72.54 m lie along the direction of bedding. At 52.43 m a quartz vein 1.9 cms wide carries tourmaline and pale green copper secondaries. Tin is indicated by PIF analysis of this vein. Quartz and tourmaline are associated in veins at 54.56 and 56.63 m. Where quartz veining occurs the bedding often appears folded and disturbed, e.g. 57.30–57.60 m. At 65.53 m a black crystalline vein 3 mm in width carrying cassiterite and tourmaline cuts the bedding at 45° (parallel to core axis). Another quartz tourmaline vein at 65.84 m shows no evidence of tin mineralisation	23.77	72.54
Fault?	Silty clay band with broken slate fragments — poor recovery	0.61	73.15
Banded slate As Cu As Sn	Hard, banded slates, dark grey in colour, broken in places, with iron staining on fracture surfaces and manganese staining around quartz veins. At 74.68 m quartz, tourmaline and arsenopyrite are associated. The quartz veins vary from 9 mm to 25 mm in width and occur both parallel with and cross-cutting the bedding. Folding of the slates is common. Copper secondaries occur with quartz at 75.29 and 76.81 m. Arsenopyrite occurs as discrete veins in proximity to quartz at 75.29, 77.11 and 80.16 m. At 81.69 m black cassiterite, quartz and mica are seen in association	9.15	82.30

Borehole 1 continued

Classification	Description	Thickness (m)	Depth (m)
Grey Slate	Broken to 85.20 m but more compact below. Quartz veins at 82.30, 83.36 and 84.12 m. Iron and manganese staining on broken faces.		
Sn	Cassiterite at 82.32 m	6.09	88.39
Banded slate	Highly folded, banded grey slates with much quartz veining. Iron staining accompanies many quartz veins and tourmaline occurs with quartz at 90.37 m. Veinlets of pyrite with		
Cu	specks of chalcopyrite are seen at 92.66 m, 97.84, 100.89 and 106.53 m. Cluster of pyrite crystals at 106.98 m	24.39	112.78
Banded siliceous slate	Light and dark grey banded rock with darker bands much harder than lighter ones. Slightly green colouration. Quartz at 113.08 m	0.61	113.39
Grey slate	Pale grey slate with chloritic coatings on fracture faces. At 113.99 m pyrite is seen on a fracture surface. Quartz veining and folding occur throughout the section. Pyrite and		
Cu	chalcopyrite are associated with quartz at 117.65 and 118.41 m. Irregular pockets of pyrite occur at 119.48 and 120.10 m	8.53	121.92

End of borehole

Borehole 2

OVERBURDEN	Slurry of slate and quartz chippings	18.59	18.59
MEADFOOT BEDS Altered slates	Red and yellow brown argillaceous slate. Much iron staining on joint facies. Small quartz veins at 23.47 and 23.77 m	5.49	24.08
Grey slate	Pale grey slate with iron and manganese oxide staining on many broken surfaces. Quartz veins of varying sizes occur at 28.65, 29.26, 29.71, 31.09, 31.70, 37.80, 38.71, 38.95, 41.76 − 42.06, 44.80 − 50.60, 45.72, 53.64, 54.56, 54.86 and 62.48 m.		
Sn	Mica and cassiterite are seen in association with the quartz at 31.70 m. Iron staining at 33.53 m. Black tourmaline vein at 39.01 m. Between 42.06 and 50.50 m the slates are intensely folded with a profusion of small quartz veinlets cutting them. At 54.25 m radiating crystals of tourmaline associated with muscovite are visible on broken surfaces of the slate. Pyrite and mica are occasionally seen on some surfaces with tourmaline	39.32	63.40

Borehole 2 continued

Classification	Description	Thickness (m)	Depth (m)
Banded slate	Pale to dark grey banded slate with quartz veining at 66.45 and 66.75 m. Disseminated pyrite is seen at 63.70 m	6.09	69.49

Grey slate
 	
As
	Broken grey slate with much quartz veining. The veins between 70.71 and 71.93 m are parallel with the bedding, whereas at 74.98 m they cut across folded slates. The slates are intensely folded and iron stained at 76.81 m.
	   The slates are indurated around quartz veins. Bedding is prominently displayed throughout the section and cleavage is well developed along bedding (80–90° to core axis) at 84.73 – 87.17 and 89.61 – 94.98 m.
	   Pyrite occurs with quartz at 89.00 m and in association with quartz and arsenopyrite at 91.44 m
		24.99	94.48

Banded siliceous slate
 	
Sn
Cu
 	
As
 	
Cu
 	
Cu
	Pale grey banded slate with bedding at 45° to core axis. These slates are harder and more silicified than those above, with quartz veins parallel to bedding.
	   At 94.80 m a vein containing prominent cassiterite crystals with pyrite and some chalcopyrite cuts the slates at 40° to core axis. A similar vein at 96.93 m carries arsenopyrite in a quartz/mica matrix with minor tourmaline present.
	   Other quartz veins at 100.89 and 102.11 m carry pyrite.
	   Specks of chalcopyrite and pyrite occur with tourmaline at 103.02 and 103.63 m and chalcopyrite is seen as veinlets within quartz at 105.46 m
		11.29	105.77

Calc-flinta	Highly altered grey to green calc-silicate rock. Banding is at 80° to core axis with green chloritic bands predominantly displayed	3.96	109.73
	Grey calc-silicate rock. Joints coated with calcite crystals at 110.19 m. At 110.64 m a quartz vein cuts the calc-flintas. This section is alternately fresh and more altered with iron staining at 117.35 m colouring the rock red. At 117.36 m the calc-silicates have been completely broken down to a clay band 7.6 cm in width. Broken quartz fragments at 118.30 m	8.84	118.57
Sn	Green calc-silicate rocks cut by many calcite-filled joints. At 119.48 m a skarn-like band 2.5 cm in width contains axinite and brown cassiterite. The core contains more chloritic banding below 120.10 m and is broken and shot through by a profusion of calcite and quartz veinlets. The lower 0.6 m of the section display hematitic veining	4.26	122.83

Borehole 3

Classification	Description	Thickness (m)	Depth (m)
Argillaceous slate	Soft grey or yellow slates heavily stained by oxidation. Tourmaline veins are common with one 15 cms in width at 67.67 m	10.36	72.54
Silicified slate	Slates invaded by many quartz veins. The slates are hard and vughy with quartz and siderite forming cavity fillings. Tourmaline forms veinlets and fracture coatings	7.01	79.55
Ferruginous slate	Highly reddened ferruginous slates with cleavage at 90° to core axis and a layering at 60° to core axis. Tourmaline bands present at 82.19 m	3.36	82.91
Grey slate Cu	Grey layered slates with a marked silica-rich zone from 85.65 to 87.48 m. The slates are highly indurated around the quartz veins and iron staining is visible on joint faces. Folded slates at 87.78 m are blackened in colour by the presence of tourmaline bands. At 90.53 m a quartz vein is associated with very minor amounts of green copper secondaries	8.23	91.14

End of borehole

APPENDIX II *DETAILS OF CORE SAMPLING*

Sample No.	BH	Depth (m)	Comments
XMD 1	1a	6.71— 7.62	Top of calc-silicate layer
2	1a	7.62— 8.23	Decomposed calc-silicate rock
3	1a	11.89— 13.41	Top of slates, some quartz veining
4	1a	30.18— 30.78	Base of grey slates, no veining
5	1a	31.69— 32.61	Top of calc-silicate layer
6	1a	39.32— 41.15	Slates with Cu secondaries at bottom of BH
7	1	18.28— 19.35	Top of slate core, weathered
8	1	34.75— 35.66	Heavily iron-stained slate; PIF indicates some Sn
9	1	37.49— 38.40	Slate; green Cu secondaries; PIF indicates Sn
10	1	50.90— 51.51	Slate with no apparent mineralisation
11	1	52.43— 52.73	Quartz vein with Cu secondaries; PIF indicates Sn
12	1	58.52— 59.44	Iron stained slate
13	1	65.23— 65.53	Tourmaline vein with cassiterite
14	1	74.98— 75.29	Cu/As in quartz veined slate
15	1	77.11— 77.42	Arsenopyrite veinlets in slate
16	1	81.38— 81.67	Quartz veining in slate
17	1	82.30— 82.91	Quartz veining in slate, traces of cassiterite
18	1	86.56— 86.87	Slate veined by quartz, some cassiterite
19	1	92.36— 92.66	Pyrite and chalcopyrite in quartz veins in slate
20	1	97.84— 98.15	Pyrite-chalcopyrite-quartz veining in slates
21	1	106.38—106.67	Pyrite-chalcopyrite-quartz veining in slates
22	1	111.56—111.86	Slate with no apparent mineralisation
23	1	117.65—118.26	Slate veined by quartz-pyrite-chalcopyrite
24	2	18.59— 19.51	Top of slate core, weathered
25	2	29.57— 29.87	Slate with quartz veining
26	2	31.70— 31.85	Slate with quartz veining, some cassiterite and mica
27	2	48.15— 48.77	Slate veined by quartz, some chalco-pyrite and arsenopyrite
28	2	53.34— 53.95	Slate with few quartz veins
29	2	87.43— 88.09	Slate with no apparent mineralisation
30	2	91.14— 91.44	Slate with quartz-arsenopyrite vein
31	2	94.50— 94.80	Cassiterite-pyrite-chalcopyrite vein in slate
32	2	96.62— 96.93	Arsenopyrite veining in slate
33	2	103.02—103.63	Traces of chalcopyrite in tourmaline veined slates
34	2	106.07—106.68	Altered, chloritic calc-silicate rock
35	2	119.18—119.79	Axinitic skarn with cassiterite
36	2	121.92—122.53	Calc-silicate rock with hematite veining
38	3	19.50— 20.12	Top of slate core, weathered and iron stained
39	3	36.58— 36.88	Iron stained slate; minor Sn indicated by PIF

Sample No.	BH	Depth (m)	Comments
40	3	51.81— 52.43	Silicified slate; PIF indicates minor Sn
41	3	65.84— 66.75	Slate with tourmaline veining
42	3	81.38— 81.99	Ferruginous slate apparently not mineralised
43	3	90.53— 90.83	Slate cut by quartz with green Cu mineral

Borehole 2 continued

Classification	Description	Thickness (m)	Depth (m)
	Grey to black calc-silicate rocks cut by many quartz veinlets. Banding is limited to a zone 20 cm in thickness at 123.14 m. The rock is vughy in nature with quartz crystals lining the cavities	0.92	123.75
Cu	Grey green calc-silicate rock with a banding at 90° to core axis. Quartz and calcite veining is common throughout the section. At 128.02 m a small veinlet of chalcopyrite cuts the calc-silicates. Below 130.45 m the banding is highly disturbed and folded with quartz veins cutting across the layers	6.70	130.45

End of borehole

Borehole 3

OVERBURDEN	Rubble of quartz and slate fragments, partly fill used in the old quarry	19.51	19.51
MEADFOOT BEDS Argillised slate	Light brown to red argillised slates. Iron oxide staining throughout, but more intense near quartz veins at 20.73, 30.48, 38.40, 39.93, 45.72, 46.63 and 46.94 m. A less altered highly silicified section occurs at 21.03 m. Small and feathered tourmaline veins cut the slates. Folding is visible from 39.01 to 39.93 m, where oxidation has markedly reddened the slates. No visible signs of mineralisation were noted, but a PIF reading at 36.58 m indicated very		
Sn	minor tin	28.34	47.85
Sandy slate	Predominantly arenaceous section with occasional bands of more silicified slaty material. The sandy layers are light grey to yellow in colour, with minor tourmaline veinlets cutting them. Bedding is almost parallel to the core axis and the upper contact between the slate and sandy layers can be seen wedging out at 49.38 m. Iron staining is common on broken surfaces and quartz veining occurs at 50.60 and 50.90 m. More silicified slaty bands are seen from 51.82 to 52.12 and 52.43 to 52.73 m. Smaller quartz veinlets associated with tourmaline dissect the sandy layers at 54.56 m. No visible mineralisation was noted but PIF		
Sn	readings indicate minor tin at 52.20 m	9.45	57.30
Silicified slate	Extremely hard and vughy slates dissected by many quartz veinlets. Iron staining on broken surfaces. Tourmaline present as veinlets and joint coatings	4.88	62.18